colorants

MDPI

Review

BODIPY Dyes: A New Frontier in Cellular Imaging and Theragnostic Applications

Panangattukara Prabhakaran Praveen Kumar [1,*], Shivanjali Saxena [2,3] and Rakesh Joshi [2]

[1] Department of Biomedical Engineering, Institute for Quantitative Health Science and Engineering, Michigan State University, East Lansing, MI 48824, USA
[2] DARVUN, Punjab 147001, India; shivanjalisaxena@gmail.com (S.S.); ciet.rakesh@gmail.com (R.J.)
[3] NYU Grossman School of Medicine, New York, NY 10016, USA
* Correspondence: pananga1@msu.edu or p4praveen.18@gmail.com

Abstract: BODIPY (Boron-Dipyrromethene) dyes have emerged as versatile fluorescent probes in cellular imaging and therapeutic applications owing to their unique chemical properties, including high fluorescence quantum yield, strong extinction coefficients, and remarkable photostability. This review synthesizes the recent advancements in BODIPY dyes, focusing on their deployment in biological imaging and therapy. The exceptional ability of BODIPY dyes to selectively stain cellular structures enables precise visualization of lipids, proteins, and nucleic acids within live and tumor cells, thereby facilitating enhanced understanding of biochemical processes. Moreover, BODIPY derivatives are increasingly utilized in Photodynamic therapy (PDT) and Photothermal therapies (PTT) for targeting cancer cells, where their capability to generate cytotoxic reactive oxygen species upon light activation offers a promising approach to tumor treatment. Recently, BODIPY derivatives have been used for Boron Neutron Capture Therapy (BNCT) for various tumors, and it is a growing research field. Advancements in nanotechnology have allowed the fabrication of BODIPY dye-based nanomedicines, either alone or with the use of metallic nanoparticles as a matrix offering the development of a new class of bioimaging and theragnostic agents. This review also discusses innovative BODIPY-based formulations and strategies that amplify therapeutic efficacy while minimizing adverse effects, underscoring the potential of these dyes as integral components in next-generation diagnostic and therapeutic modalities. By summarizing current research and future perspectives, this review highlights the critical importance of BODIPY dyes in advancing the fields of cellular imaging and treatment methodologies.

Keywords: BODIPY dye; cellular imaging; photodynamic therapy; photothermal therapy; boron neutron capture therapy

check for updates

Academic Editor: Anthony Harriman

Received: 23 January 2025
Revised: 18 March 2025
Accepted: 20 March 2025
Published: 02 April 2025

Citation: Kumar, P.P.P.; Saxena, S.; Joshi, R. BODIPY Dyes: A New Frontier in Cellular Imaging and Theragnostic Applications. *Colorants* **2025**, *4*, 13. https://doi.org/10.3390/colorants4020013

Copyright: © 2025 by the authors. Licensee MDPI, Basel, Switzerland. This article is an open access article distributed under the terms and conditions of the Creative Commons Attribution (CC BY) license (https://creativecommons.org/licenses/by/4.0/).

1. Introduction

BODIPY dyes, or boron-dipyrromethene compounds (IUPAC name 4,4-difluoro-4-bora-3a,4a-diaza-s-indacene), have shaped the landscape of fluorescent imaging and bio-analytical applications since their inception [1–3]. The synthesis of the first BODIPY dye in 1968 by chemists Treibs and Kreuzer marked the beginning of an era characterized by their remarkable optical properties, including high fluorescence quantum yields and strong absorption in the visible and near-infrared spectra [4]. A general synthetic scheme for BODPY dye using pyrrole and benzaldehyde is represented in Figure 1A [5]. The method involves condensing an aromatic aldehyde with a pyrrole (having a free α-position) using an acid catalyst, typically trifluoroacetic acid. This forms an unstable pyrrolylcarbinol,

which undergoes protonation, dehydration, and mesomeric stabilization to yield an azafulvenium ion. A second pyrrole then attacks, forming an intermediate that deprotonates into dipyrrolylmethane. This is oxidized in situ to dipyrrolylmethene, followed by the addition of a base (usually a tertiary amine) and BF_3OEt_2. A detailed mechanistic pathway is shown in Figure 1B for these procedures. Recent advancements in synthetic procedures offer various substrates, such as acid chlorides as a precursor for conjugation of pyrrole derivatives. These procedures lack the oxidation steps and offer clean work up procedures for purification. Owing to excellent photophysics, BODIPY dyes are invaluable in biological research, particularly in fluorescence microscopy, cell imaging, and protein labeling [6–8]. Over the years, innovative approaches to modifying BODIPY structures have expanded their applications, allowing them to serve as effective probes for various biological processes, therapeutic agents, and biosensors. As a result, BODIPY dyes have gained significant attention for their potential in cancer therapies and diagnostic applications due to their tunable properties, photostability, and low toxicity, which are crucial for in vivo imaging and the monitoring of dynamic biological events. The present review will explore the historical development of BODIPY dyes, highlighting their journey from laboratory discovery to a pivotal role in advancing biomedicine through their diverse applications in contemporary biological research.

The modification of BODIPY dyes has enhanced their versatility, enabling researchers to customize their properties for specific biological tasks, including sub-cellular imaging and targeted therapy [8–10]. A significant breakthrough in this field is the introduction of aza-BODIPYs, which are formed by substituting the meso-carbon atom of the traditional BODIPY structure with a nitrogen atom (aza-N). This substitution markedly improves their photophysical characteristics. Figure 1C represents a general schematic for the structure of various BODIPY, Aza-BODIPY, and substituted BODIPY dyes. Unlike standard BODIPYs that primarily emit green light, aza-BODIPYs can absorb and emit light in the red to near-infrared spectrum (Figure 1D) [11]. Although these compounds generally exhibit lower emission quantum yields, they have an increased propensity for intersystem crossing (ISC) to triplet states, rendering them particularly effective for applications that depend on triplet state processes, such as Photodynamic therapy [12–15].

Using fluorescent probes that operate within the NIR-II window presents several advantages for bioimaging, including minimized light scattering, enhanced tissue penetration, improved signal-to-background ratios, and better spatiotemporal resolution. BODIPY dyes are particularly advantageous due to their exceptional photostability, elevated quantum yield, narrow absorption profiles, straightforward functionalization, and low cytotoxicity. The integration of these traits into BODIPY probes that are functional in the NIR-II window holds tremendous promise for bioimaging applications (Figure 1E). As Hu et al. note, pivotal strategies for achieving this goal include electron pumping, conjugation with semiconducting polymers, and the formation of J-aggregates [16]. Each of these strategies, however, comes with its own set of advantages and challenges. The electron pumping approach utilizes an electron-withdrawing BODIPY core that can effectively incorporate electron-donating groups, thereby enhancing the tunability of the emission wavelength while maintaining photostability. The primary challenge with this method lies in reconciling these emission traits with the overall brightness of the fluorescence [17–21]. Conversely, several research teams have investigated the incorporation of BODIPY units into semiconducting polymers, which facilitates the integration of multiple functions in a single system. However, the complexity often leads to limitations in clinical applicability and can reduce the brightness of such dyes [22–24]. Similarly, the formation of J-aggregates takes advantage of the specific arrangement of stacked BODIPY molecules, offering substantial benefits such as minimal structural modifications and high fluorescence quantum yields which

contribute to superior imaging signals [25]. Nonetheless, this method faces difficulties with the stability of the aggregates and challenges linked to achieving in situ formation of NIR-II J-aggregates within biological contexts like tumors [26–28]. The fluorescence of BODIPY molecules can be controlled by various pathways such as Photoinduced electron transfer (PET), Förster resonance energy transfer (FRET), Intramolecular Charge Transfer (ICT), and various other pathways [29,30].

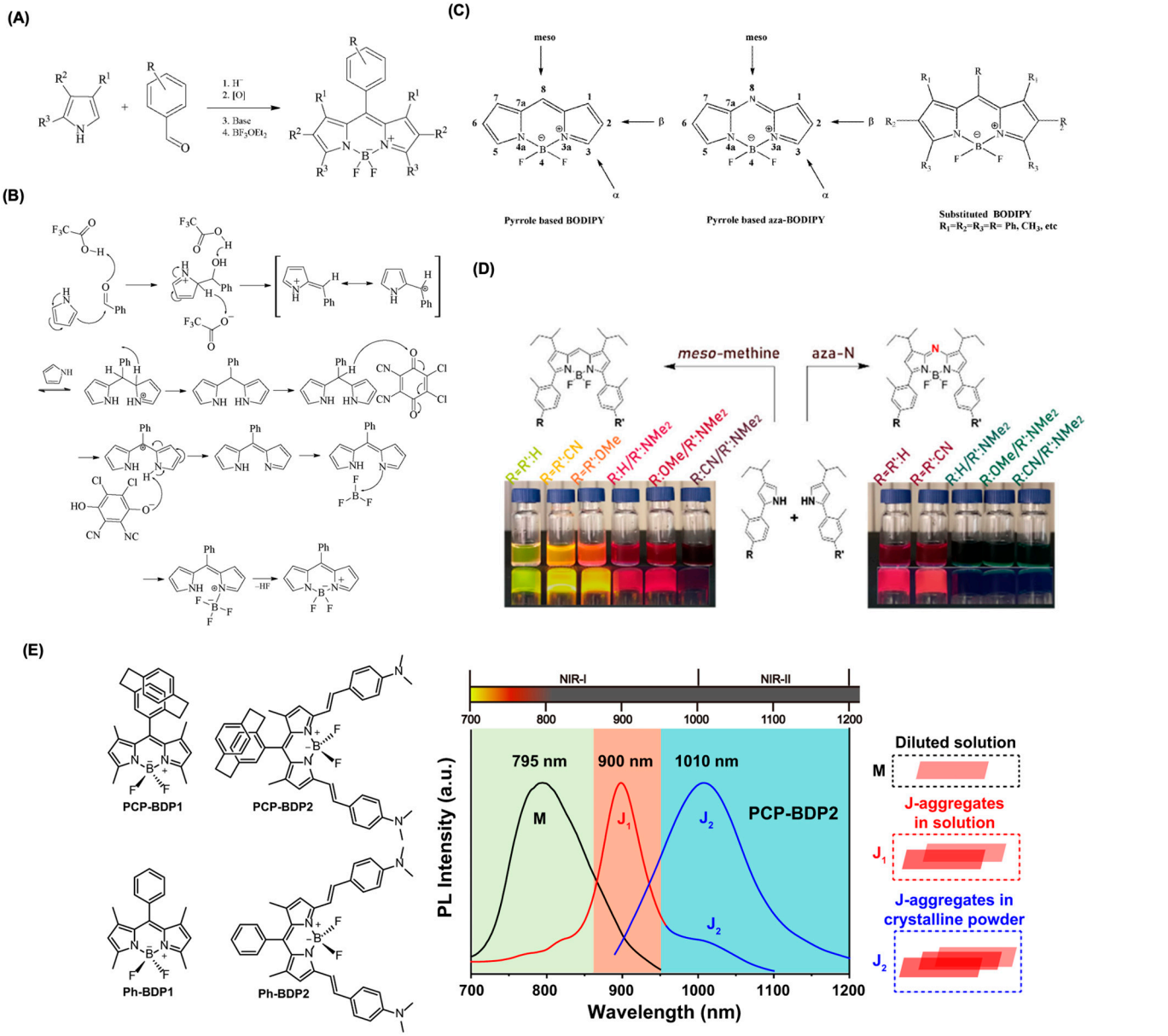


Figure 1. (**A**,**B**) General synthetic route for BODIPY dye formation and a mechanistic pathway for the formation of BODIPY. (**C**) A representation for the general core structure of BODIPY, aza-BODIPY and substituted BODIPY dyes. (**D**) Structure of substituted BODIPY and aza-BODIPY dyes and a picture of the fluorescence from these dyes with varying substituents. (**E**) Structural representation of NIR-II active BODIPY dye and their J-aggregates with tunable absorption and emission properties. Reproduced with permission from [11], 2022, ACS, and [25], 2021, Nature publishing group.

BODIPY dyes have emerged as vital components in the development of small-molecule fluorescent probes, attributed to their remarkable photophysical properties. Unlike fluorescent proteins, which can be bulky and challenging to manipulate, BODIPY dyes are significantly smaller, facilitating their use in biological contexts without interfering with the

functionality of target molecules. This unique advantage allows for more effective bioimaging and molecular interactions. Moreover, BODIPY dyes can undergo fine-tuning through chemical modifications to create various derivatives tailored for specific biomolecular interactions or for localization within distinct cellular compartments.

Recent advancements show promise in engineering BODIPY-based probes for targeted localization within cellular organelles such as mitochondria, lysosomes, the Golgi apparatus, lipid droplets, and the endoplasmic reticulum. These probes are designed with high selectivity and specificity, making them particularly suitable for exploring subcellular dynamics and interactions. For instance, probes intended for mitochondrial imaging are formulated to be positively charged, allowing them to navigate into the negatively charged organelle while minimizing background fluorescence, thus enhancing imaging accuracy. Innovations aimed at enhancing the water solubility and membrane permeability of BODIPY derivatives have expanded their applicability in live-cell imaging, overcoming previous limitations related to solubility.

In addition to their utility in imaging, BODIPY dyes show promising applications in therapeutic contexts, particularly in Photodynamic therapies (PDT) where BODIPY dyes act as photosensitizers that generate cytotoxic reactive oxygen species upon light activation, targeting specific cell types effectively [31]. By extending the conjugation of BODIPY molecules, researchers have achieved superior photothermal conversion efficiencies exceeding 90%, which is essential for effective energy absorption during Photothermal therapy (PTT) [32]. These attributes position BODIPYs as versatile agents in cancer therapies that utilize light-induced mechanisms to eradicate tumor cells. Recently, BODIPY derivatives have been attached to sodium borocaptate (10B-BSH) for Boron Neutron Capture Therapy (BNCT) for tumors.

BODIPY molecules typically exhibit low water solubility, which poses challenges for in vivo administration and limits their accumulation in solid tumors. Thankfully, advancements in nanotechnology and supramolecular chemistry have introduced strategies to enhance the delivery and tumor-targeting capabilities of BODIPY dyes through nanomedicine formulations [33,34]. This progress has established a foundation for ongoing research in cancer theragnostic, offering significant potential for clinical applications.

The present review offers a critical assessment of the structural design of BODIPY-based theranostic agents and their applications in bioimaging and cancer therapy, particularly those described in the last 7 years. The use of various targeting conjugates on the backbone of BODIPY dyes allowed localization of the dyes inside the tumor and cellular components, which allowed tracking of these cell features using various imaging modalities such as fluorescence microscopy, confocal microscopy, Raman and Photoacoustic imaging. We covered the features of BODIPY dyes as therapeutical drugs for PDT, PTT, and BNCT-based tumor ablation studies. With the wide application of nanoparticle formulations, the use of BODIPY based nanomedicines was also covered in the review article.

Finally, this article offers fresh perspectives on BODIPY dyes, delving into their photophysical characteristics and potential clinical applications. It examines critical clinical factors, such as the regulation of related proteins and pertinent challenges. The review also highlights ongoing and future clinical trials. By providing a detailed exploration, this discussion seeks to enhance the audience's understanding of the progress in utilizing BODIPY dyes for subcellular imaging and therapeutic innovations. Moreover, these insights emphasize the ongoing role of BODIPY dyes in advancing diagnostic and therapeutic strategies within the biomedical field. Figure 2 represents the application of BODIPY dye in various fields, such as utilization as a fluorescent sensor, a bioimaging tool, and in therapeutical applications.

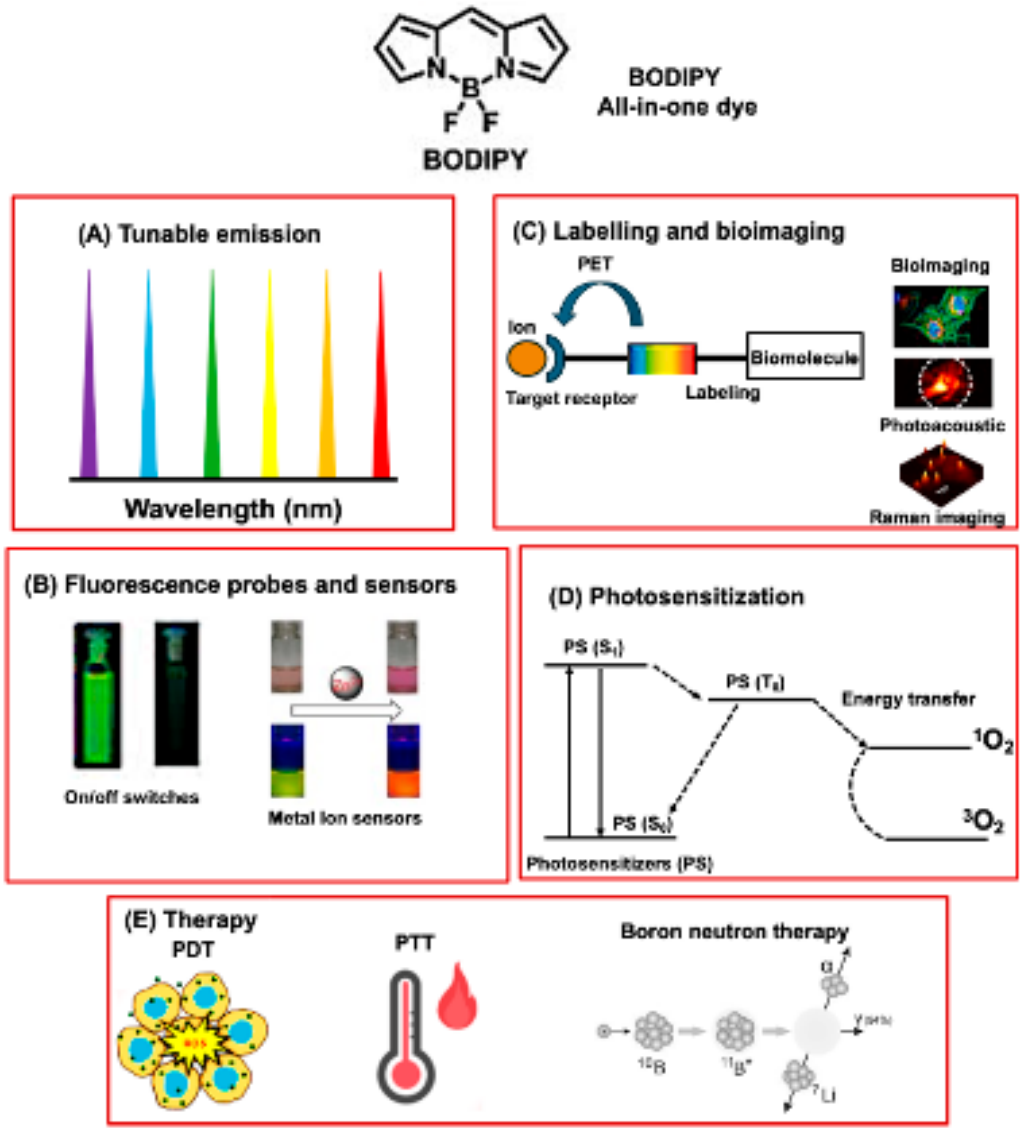


Figure 2. Application of BODIPY dye as a fluorescent sensor (**A**,**B**), bioimaging tool (**C**), and as a therapeutical material (**D**,**E**), respectively.

2. Mechanisms of Intracellular Distribution of BODIPY Dyes

BODIPY compounds' intracellular distribution plays a vital role in their applications in bioimaging and therapy. Their structural and physicochemical properties influence localization within cells, such as in the plasma membrane, cytoplasm, endoplasmic reticulum, mitochondria, lysosomes, and Golgi apparatus. For instance, unmodified, lipophilic BODIPY dyes integrate into lipid-rich membranes, making them ideal for staining the plasma membrane and endoplasmic reticulum, though they lack specificity for organelles. Functionalizing BODIPY dyes enables targeted subcellular localization; positively charged groups like PPh_{3+} help target mitochondria due to its negative membrane potential. Lysosomal probes are designed with groups that protonate in acidic environments, ensuring retention. Similarly, amphiphilic modifications facilitate plasma membrane localization, while hydrophilic properties enhance cytoplasmic retention. BODIPY and its unique characteristics enable the visualization of intricate biological processes, including lipid metabolism, membrane dynamics, and protein localization (BODIPY Dye Series—Section 1.4 | Thermo Fisher Scientific—USA, 2024). Understanding the intracellular distribution mechanisms of BODIPY dyes is essential for accurately employing these fluorescent probes in various

research applications, from cell signaling to cancer biology [6,35]. The key mechanisms through which BODIPY dyes distribute intracellularly are by any of the following pathways: passive diffusion, endocytosis, and specific interactions with cellular components.

2.1. Passive Diffusion

One of the fundamental mechanisms of intracellular distribution for BODIPY dyes is passive diffusion through cellular membranes. The amphiphilic nature of many BODIPY dyes allows them to readily integrate into lipid bilayers. For instance, BODIPY FL-sphingomyelin analogs are designed to enter cellular membranes spontaneously, enabling the measurement of lipid trafficking and dynamics across various cellular compartments [36]. This property allows BODIPY dyes to label lipid droplets and enriched regions within the plasma membrane, thus highlighting their utility in studying lipid storage and metabolism [35]. Furthermore, the design of BODIPY dyes can influence their diffusion characteristics. For example, the addition of different fatty acid chains alters their hydrophobicity, affecting how they partition within the membrane and how readily they can diffuse into cells. Lower concentrations of BODIPY dyes may enhance diffusion efficiency, allowing for their widespread distribution in the cytoplasm and subsequent localization to organelles such as mitochondria (Figure 3A) [37].

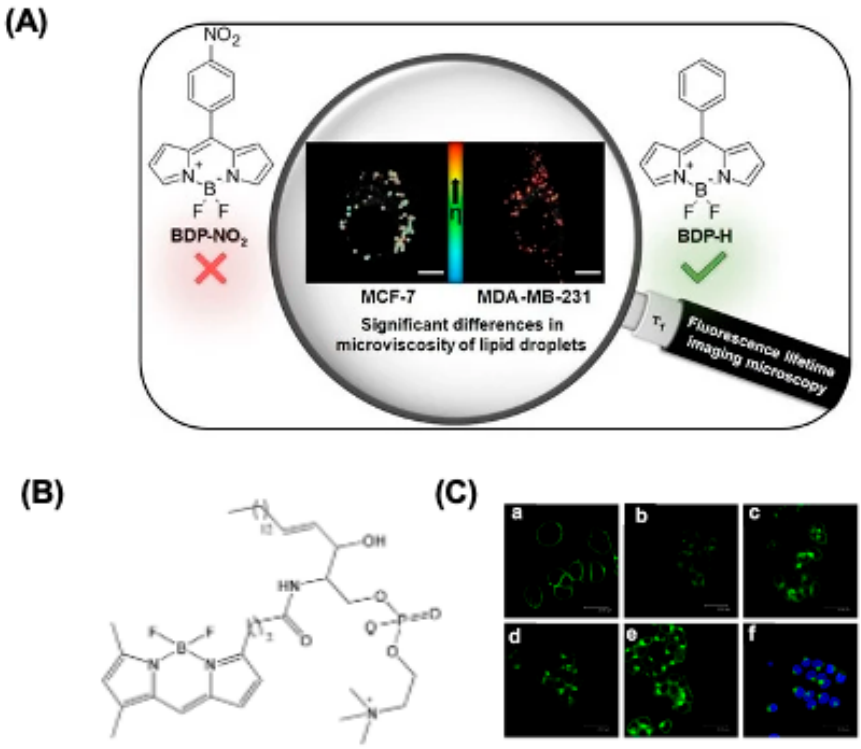


Figure 3. (**A**) Chemical structures of BODIPY dyes and their application in monitoring microviscosity in cellular environment, and effect of cellular imaging. (**B**) Chemical structure of BODIPY-sphingomyelin. (**C**) Fluorescence images showing the cellular uptake process of BODIPY-sphingomyelin into plasma membrane at different times: (**a**) 0 min, (**b**) 5 min, (**c**) 15 min, (**d**) 30 min, (**e**) 60 min, or (**f**) 240 min at 37 °C. Reproduced with permission from [37], 2022, MDPI publisher, and [38], 2013, Elsevier.

2.2. Endocytosis

Another critical process governing the intracellular distribution of BODIPY dyes is endocytosis, particularly the clathrin-mediated endocytosis and caveolar uptake mechanisms. Following internalization through these pathways, BODIPY-labeled sphingolipids can be tracked to various organelles, notably lysosomes and the endoplasmic reticulum [38].

For example, BODIPY-sphingomyelin undergoes distinct trafficking pathways, initially localizing to the plasma membrane and later to the Golgi apparatus and lysosomal compartments over time (Figure 3B,C). These advancements allow researchers to elucidate the roles of lipid signaling molecules in cellular processes, such as differentiation and apoptosis, showcasing the dyes' capabilities in studying lipid metabolism [38,39].

Moreover, the mechanism of endocytosis can vary significantly among different cell types, impacting how BODIPY dyes are taken up and utilized within the cell. For instance, in cell types with higher rates of endocytic activity, such as neural cells, BODIPY dyes might internalize more efficiently, enabling detailed imaging of endosomal pathways. Research indicates that such variability can lead to distinct spatial distributions of BODIPY dyes within cells, influencing the interpretation of intracellular imaging results.

2.3. Specific Interactions with Cellular Components

The interaction between BODIPY dyes and specific cellular components also plays a significant role in determining their intracellular distribution. Functionalization of BODIPY dyes allows for targeted localization within specific organelles or biomolecules. For example, BODIPY dyes can be functionalized to selectively bind to lipid droplets or certain proteins, which directs their accumulation to select sites within the cell [40,41]. This specificity is particularly useful when employing BODIPY dyes as indicators of cellular processes, such as monitoring changes in lipid droplet size and density in response to metabolic perturbations [42–44].

Additionally, the chemical structure of BODIPY derivatives can affect their spectral properties and the dynamics of their interactions within the cellular environment. For instance, BODIPY dyes can display different fluorescence intensities based on their localization, which can be used to analyze changes in microviscosity in distinct cellular compartments [37,45]. Such sensing properties are vital for understanding the physiological and pathological states of cells by offering insights into the biophysical properties of organelles like lipid droplets and membranes [46–48].

3. Intracellular Distribution of BODIPY Dyes

BODIPY dyes exhibit versatile partitioning properties, allowing them to distribute within various cellular compartments as shown in Figure 4. This distribution is influenced primarily by the dye's hydrophilic–hydrophobic balance, charge, and molecular size. For instance, unmodified lipophilic BODIPYs preferentially integrate into lipid-rich membranes, making them ideal for staining the plasma membrane and endoplasmic reticulum. However, due to their ability to diffuse across membranes, these dyes may stain the cytoplasm without offering specificity for intracellular organelles. Advanced targeting strategies have been developed to enhance the subcellular localization of BODIPY dyes. When aimed at mitochondria, the dye is often functionalized with positively charged groups, such as triphenylphosphonium (TPP) and quaternary ammonium groups, to exploit the negatively charged mitochondrial membrane potential. Conversely, targeting lysosomes involves using probes that remain neutral at the cytosolic pH, becoming protonated and effectively trapped in the acidic environment of the lysosomes after entry. Similarly, to interact specifically with the plasma membrane, BODIPY probes are designed to be amphiphilic, allowing them to integrate smoothly with the amphiphilic constituents of the membrane. Additionally, increasing the hydrophilicity of these probes can enhance their retention within the cytoplasm, thus improving imaging and biological analysis capabilities. Collectively, these functionalization techniques are crucial for optimizing the bioimaging capabilities and overall application of BODIPY dyes in cell biology research.

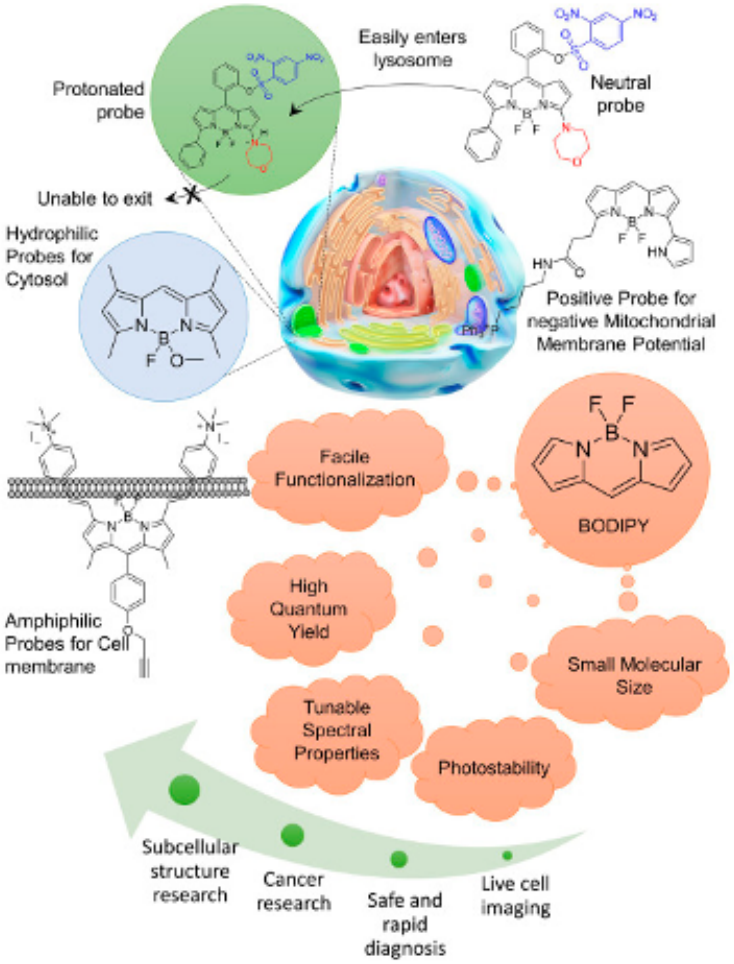


Figure 4. A general schematic representation for the structural modifications and intracellular distribution of BODIPY dyes. Reproduced with permission from [8], 2025, Elsevier.

4. BODIPY for Bioimaging Applications

4.1. BODIPY Dyes for Membrane Imaging

Design and synthesis of plasma membrane-targeted BODIPY dyes are of interest these days due to their less invasive detection methods and they are not affected by most biological events due to their versatile and robust designs [6,49–51]. For this, the backbone of BODIPY can be easily modified to make the lipophilic balance for the penetration into the plasma membrane.

In the pursuit of improving bioimaging techniques, Collot et al. developed a series of BODIPY-based probes specifically designed for efficient staining of plasma membranes (Figure 5A) [51]. This novel probe was created by functionalizing a green-emitting BODIPY fluorophore with amphiphilic, zwitterionic, and aliphatic anchors, leading to the generation of three variants possessing one to three anchors (Probe 1–3). Among these, probe (2) exhibited the highest quantum yield of 0.92, indicating its exceptional fluorescence properties. Probe (2) effectively targets the plasma membrane, existing as nonfluorescent soluble aggregates in aqueous environments that disassemble upon contact with the membrane. This mechanism results in bright fluorescence, yielding high signal-to-noise ratios and enhanced targeting capabilities compared to traditional fluorescently labeled lectins. In various bioimaging applications, including studies on KB cells, HeLa cells, and U87 glioblastoma spheroids, this probe demonstrated robust fluorescence intensity with specific absorption and emission wavelengths near 500 nm (Figure 5B). The imaging techniques utilized were confocal microscopy and two-photon excitation, with probe (2) showcasing

excellent cellular uptake efficiency and significant overlap with utilized plasma membrane markers. The fluorescence activation acts as a direct response to interactions with the plasma membrane, enabling precise monitoring of cellular components. Importantly, cytotoxicity assessments indicated low toxicity levels, while ex vivo and in vivo studies suggested favorable biodistribution and targetability.

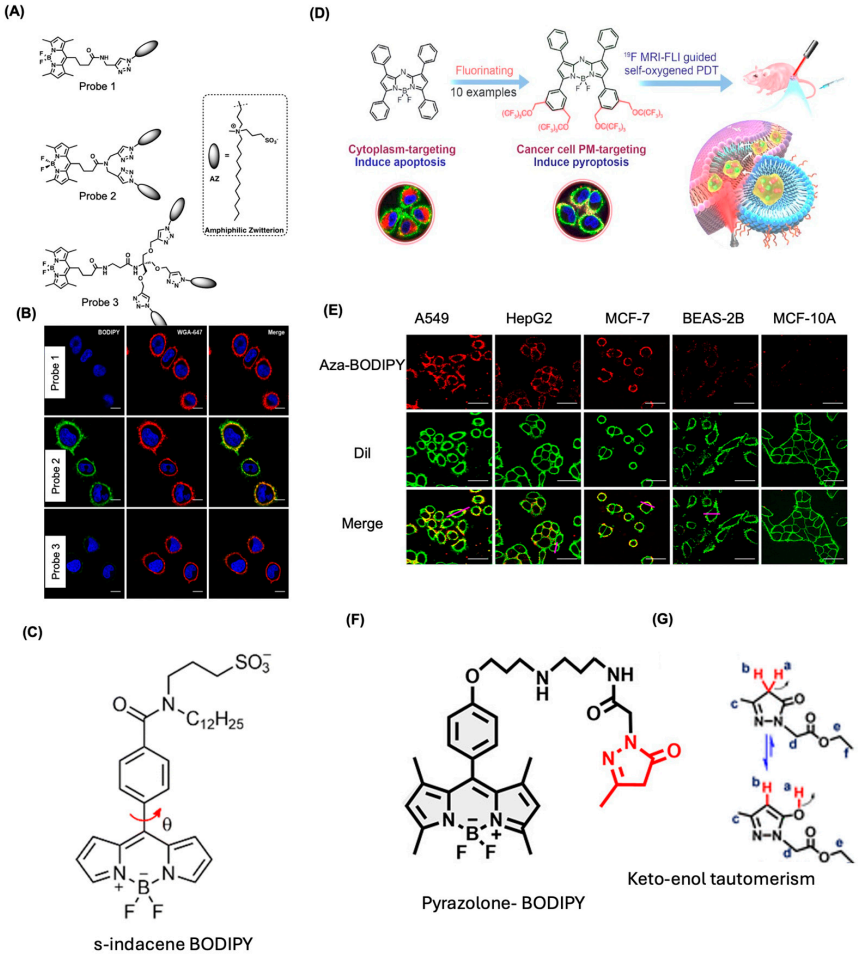


Figure 5. Designed BODIPY dyes for membrane imaging. (**A**) Structure for the amphiphilic BODIPY probe 1–3 for plasma membrane imaging applications. (**B**) The confocal laser scanning microscopy images of KB cells treated with amphiphilic BODIPYs probes 1–3, (20 nM) without any washing steps. The images were recorded 10 min after the dye application. WGA-647 (2 μg/mL), a far-red-emitting lectin, was employed to colocalize the plasma membrane, while the nucleus was pre-stained with Hoechst (5 μg/mL) before imaging. All images were acquired and processed under consistent settings, with a scale bar representing 15 μm. (**C**) Chemical structure for the viscosity-sensitive s-indacene BODIPY probe. (**D**) A schematic representation for the fabrication of aza-BODIPY dye for fluorescence and MRI based imaging applications. (**E**) Confocal microscopic images for the aza-BODIPY dye for various cell lines. (**F**) Chemical structure for pyrazolone BODIY for bioimaging application. (**G**) Keto-enol tautomerism for pyrazolone moiety. Reproduced with permission from [51,52], 2019, 2025, ACS, respectively.

In one of the studies, Polita et al. fabricated a viscosity-sensitive s-indacene BODIPY probe for plasma membrane viscosity imaging (Figure 5C) [50]. Fluorescence lifetime imaging results showed that these probes can stain A549 live lung cancer cells within 5 min and the slow internalization allowed for monitoring of the cytoplasm viscosity. Li et al. fabricated an aza-BODIPY system as a bioimaging agent for the plasma membrane of A549 cells (Figure 5D) [52]. To improve the targeting and internalization, the BODIPY core is conjugated with fluorine atoms, and this probe is used for both fluorescence

and MRI-based bioimaging applications (Figure 5E). The fluorine-19 MRI allowed the detection of oxygen delivery and oxygen partial pressure during PDT studies. Through comparative physicochemical and biological analyses, supported by molecular dynamics simulations, it has been shown that fluorinated BODIPY can act like photosensitizers that specifically target and eliminate cancer cells. This occurs through the oxidation of plasma membrane phospholipids by singlet oxygen ($^1O_2$), triggering pyroptosis. This mechanism effectively inhibits tumor progression when used in self-oxygenating ^{19}F MRI-FLI-guided photodynamic therapy in mice. The findings highlight a fluorination strategy to develop high-performance, multifunctional materials that precisely target cancer cell membranes, paving the way for advancements in cancer treatment and related applications.

Xiong et al. studied pyrazolone-functionalized probes for bioimaging and therapy, focusing on Nile blue, rhodamine, and BODIPY derivatives (Figure 5F) [53]. The BODIPY derivative showed strong potential for subcellular imaging and therapeutic use. It was designed to target cell membranes, with the pyrazolone moiety enabling stable interactions with membrane proteins through noncovalent bonds with amino acids like arginine. The pyrazolone group's ability to tautomerize into its enolic form ensured prolonged fluorescence signal retention, making the derivative effective for long-term imaging (Figure 5G). The BODIPY-pyrazolone probe exhibits strong fluorescence (excitation at 488 nm, emission at 490–540 nm), enabling high-resolution, stable, and photobleaching-resistant imaging of cell membranes for over 96 h. The probe showed selective binding to membrane proteins, without cell penetration, making it suitable for long-term monitoring, targeted delivery, and diagnostic applications, particularly in cancer. Among the various scaffolds studied, the BODIPY derivative stands out for its robust photophysical properties and potential in subcellular imaging and membrane-targeted therapies, enriching the toolkit of BODIPY-based bioimaging agents.

BODIPY dyes have emerged as indispensable tools in the field of membrane imaging, providing researchers with robust and versatile options for studying cellular membranes. While challenges such as fluorescence quenching and dye synthesis complexities exist, ongoing advancements in dye development and imaging techniques continue to enhance the efficacy of BODIPY dyes in biological research. As a result, they are likely to remain a fundamental component of molecular imaging strategies aimed at unraveling the intricate dynamics of biological membranes.

4.2. BODIPY Dyes for Cytosol Imaging

BODIPY-based molecular rotors have gained prominence for measuring intracellular microviscosity, a critical parameter influencing cellular behavior and the diffusion of biomolecules. The technique leverages the property that BODIPY dyes respond to varying viscosities in their environment; the intramolecular rotation of the dye is hindered in a highly viscous medium, resulting in increased fluorescence intensity and a longer fluorescence lifetime [37,54]. Studies have shown that different BODIPY dyes retain stability in aqueous solutions, allowing for effective monitoring of microviscosity in the cytosol of live cells, including aggressive cancer cell lines such as MDA-MB-231 [37]. This capability has profound implications for understanding cellular dynamics and disease mechanisms.

In 2014, Courtis et al. developed monoalkoxy-BODIPY probes (probe 4), known as MayaFluors, with improved bio-imaging features (Figure 6A) [55]. The synthesis used a simple two-step process, starting with difluoro-BODIPY activation to form a BODIPY-OTf intermediate, followed by alcohol addition. The structure retains one fluorine atom, allowing property fine-tuning and modifications like methoxy (probe 4), glycol (probe 5), NHS-ester (probe 6), and tetrazine (probe 7) to enhance functionality and targetability. MayaFluors (the common name for these dyes) demonstrated efficient membrane permeability, minimal nonspecific binding, and superior performance compared to other

strategies. Tested on MD-MBA-231 and MCF-7 cells, they showed excellent uptake with low background staining (Figure 6B). Key fluorescence properties include absorption at 490 nm, emission at 512 nm, quantum yields of 0.3–0.5, and dye stability. Colocalization and microscopy studies confirmed their specificity, while FRET-based fluorescence activation via tetrazine-tagged probes makes them ideal for cytosolic targeting.

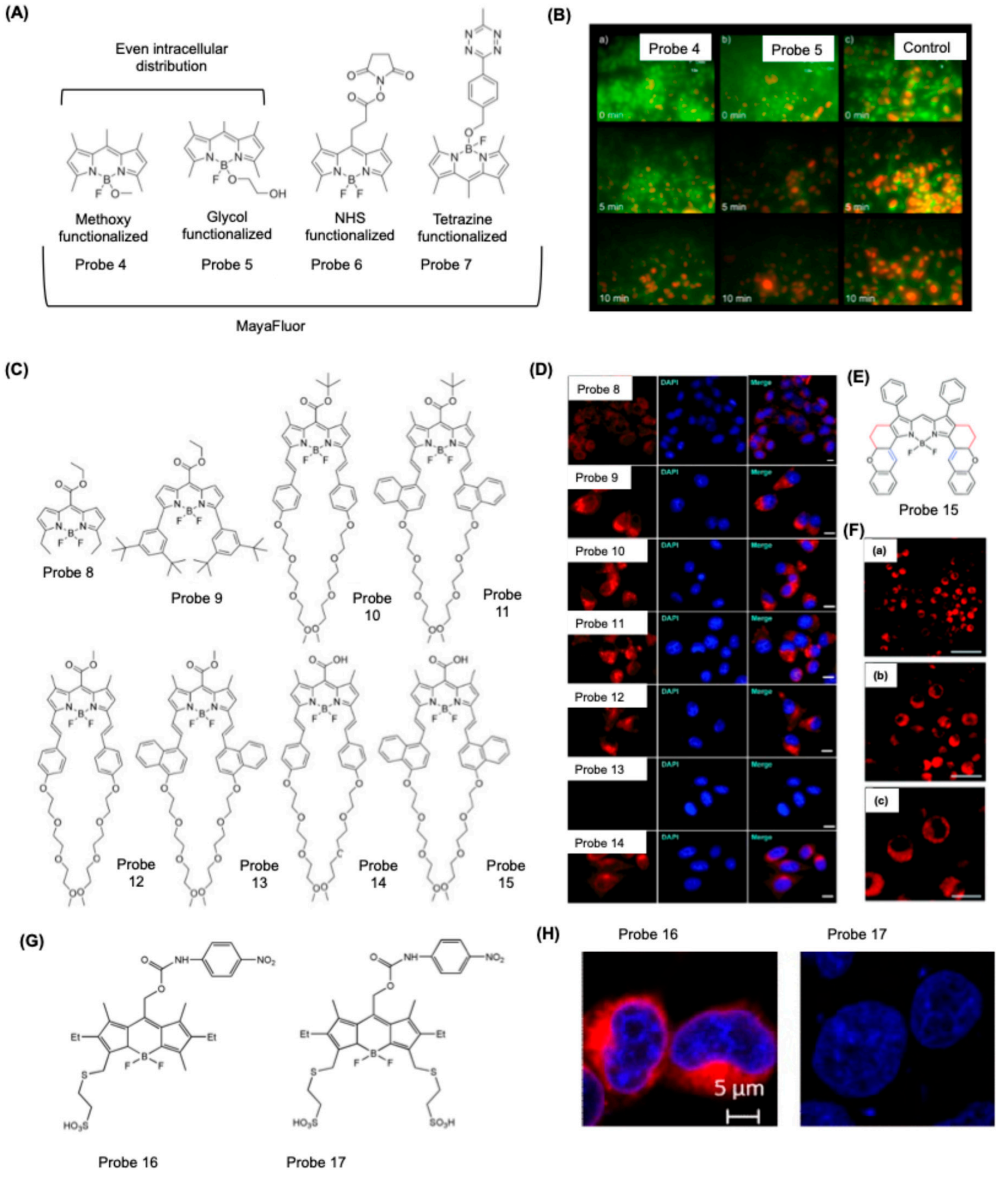


Figure 6. Synthesized BODIPY probes for Cytosol imaging. (**A**) Chemical structures for the MayaFluors probes (4–7). (**B**) Time dependent cellular uptake and intracellular distribution of probe 4, 5 and control BODIPY dye using MD-MBA 231 cells. (**C**) Structure for the BODIPY probes 8–15, with varying conjugation and water-soluble groups for bioimaging application. (**D**) Fluorescence images for the probes 8–15 using live Hela cells using 1 µM concentration of the dyes. Various emission filters are used depending on the photophysical properties of the dyes. Texas Red filter (for 8, 9), NIR filter (for 10, 11), or Cy5 filter (for 11, 13, 14). Nuclei were stained using Hoechst, and images were taken under a DAPI filter. Scale bar: 10 µm. (**E**) Chemical structure for the NIR emitting BODIPY probe 15, and (**F**) HepG2 cells imaging data using probe 15, after incubating the probe with a concentration of 2×10^{-5} M. Scale bar: (**a**) 40 µm; (**b**) 20 µm; (**c**) 10 µm. (**G**,**H**) Chemical structure and confocal fluorescence microscopy of HEK 293T cells treated with probes 16–17 for 30 min and costained with Hoechst dye. Reproduced with permission from [55], 2014, ACS; [56], 2014, European Chemical Societies publishing; [57], 2012, RSC publishing group; [43], ACS, 2020, respectively.

A series of alkene-substituted BODIPY derivatives (probes 8–15) were fabricated by Ni et al. (Figure 6C) [56]. The substitution of backbones using methyl ester and carboxylic acid groups improved the solubility, whereas the alkene substitution improved their absorbance and emission to the far red region (absorption maxima ranging from 627 nm to 682 nm, emission maxima ranging from 642 nm to 729 nm). The derivatives showed enhanced fluorescence quantum yields from 6 to 36% and showed high sensitivity and specificity towards Hela cells using fluorescence and confocal microscopy imaging (Figure 6D). Jiang et al. fabricated a NIR BODIPY probe bearing 3,4,4a-trihydroxanthene moieties for the bioimaging application (Figure 6E). The probe showed an absorption at 732 nm with an emission at 747 nm [57]. The targeting mechanism of the probe showed specificity for cellular components, particularly localizing to the cytoplasm of living HepG2 cells (Figure 6F). The probe showed a turn-on fluorescence response driven by cellular interactions, with changes linked to extended conjugation and rigidification. It holds promise for photodynamic therapy (PDT), leveraging its NIR fluorescence for deep tissue imaging and non-invasive diagnostics. Its stability and low cytotoxicity enhance therapeutic potential, though comparisons with existing treatments are lacking. In vitro studies confirmed low cytotoxicity, but in vivo research on biodistribution and efficacy is limited. While offering stability, non-cytotoxicity, and NIR imaging suitability, further in vivo validation and improved fluorescence intensity and specificity are needed.

Kand et al. developed highly water-soluble probes 16 and 17 with precise cellular localization control and favorable spectroscopic and photoreaction properties [43]. The synthesis involved sulfonating meso-methyl BODIPY photocages using 2-mercaptoethanesulfonic acid sodium salt, resulting in mono- and di-sulfonated BODIPY variants (Figure 6G, probes 16 and 17). These sulfonated groups enhanced water solubility and cellular permeability control. The mono-sulfonated BODIPY could cross the cell membrane, while the di-sulfonated version was restricted to cell-surface receptors (Figure 6H). The BODIPY structure, with its hydrophilic sulfonate groups, allowed for regulated accumulation in cells, useful in bioimaging applications for mammalian cells and neurons.

4.3. BODIPY for Mitochondria Imaging

Mitochondrial imaging has gained considerable attention due to the organelle's critical roles in cellular metabolism, signaling, and overall health. BODIPY dyes, characterized by their unique photophysical properties, have emerged as powerful tools for imaging mitochondria in live cells. These dyes offer high photostability, brightness, and versatility, making them suitable for various imaging techniques, including fluorescence microscopy. The structural versatility of BODIPY dyes allows for modifications that can enhance their specificity and sensitivity toward mitochondria. Their high fluorescence quantum yields and stability mean that they emit bright signals, which are critical for effective imaging applications. One of the main advantages of BODIPY dyes is their ability to be fine-tuned for specific applications through structural modifications. For example, the introduction of lipophilic cations, such as triaryl phosphonium (TPP+), facilitates the accumulation of these dyes within the mitochondrial matrix, exploiting the negative mitochondrial membrane potential. This characteristic enhances the effectiveness of BODIPY dyes in assessing mitochondrial function and health.

Recent advancements have led to the development of various BODIPY-based probes specifically designed for mitochondrial imaging. For example, BODIPY-Mito-1 to BODIPY-Mito-6 have been synthesized to exhibit high sensitivity to changes in the mitochondrial membrane potential, allowing for real-time monitoring of mitochondrial dynamics (Figure 7A) [49]. Among these, BODIPY-Mito-6 was particularly noted for its efficacy, showing a reduction in emission intensity of up to 75% upon mitochondrial depolariza-

tion, indicating its strong potential for studying mitochondrial health and viability. The incorporation of poly(ethylene glycol) chains into BODIPY dyes has been explored to improve biocompatibility. This modification enhances the overall stability of the dyes and reduces cytotoxicity without compromising their ability to target mitochondria (Figure 7B). Furthermore, these probes have demonstrated excellent localization in mitochondria, as evidenced by high Pearson's correlation coefficients when co-stained with commercially available mitochondrial markers (Figure 7C).

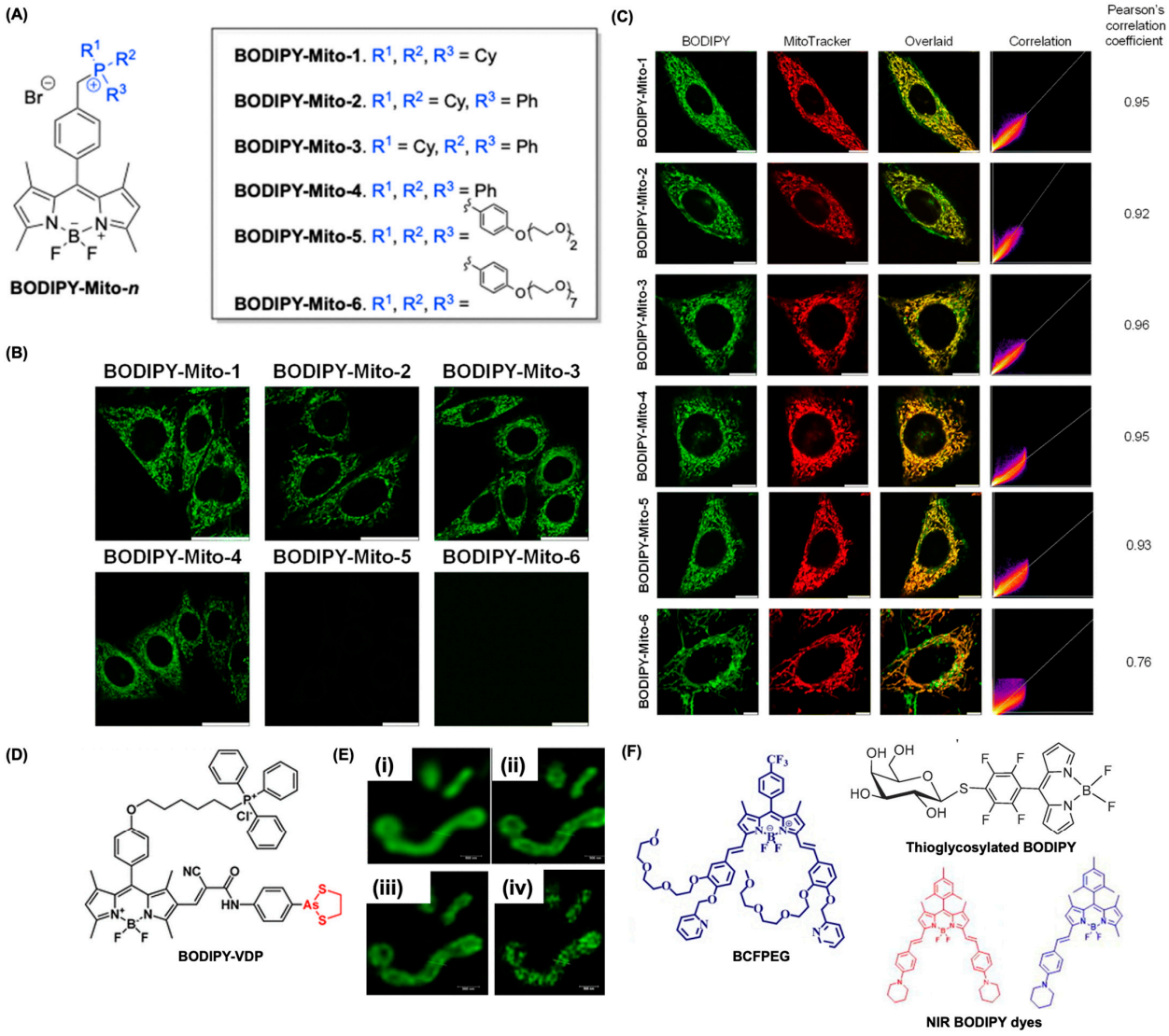


Figure 7. Mitochondria targeting BODIPY dyes. (**A**) Chemical structures for the mitochondria targeting BODIPY-Mito dyes with phosphonium groups. (**B**) Laser-scanning confocal microscopy images for the BODIPY-Mito dyes using HeLa cells as model system. Scale bar = 25 µm. (**C**) Laser-scanning confocal microscopy images for fabricated BODIPY-Mito dyes, and Mito Tracker with their Pearson's correlation coefficient. Studies showed that cyclohexyl and phenyl moieties attached with the phosphonium groups can realize high accumulation of the probes in the mitochondria. Scale bar = 10 µm. (**D**) Chemical structure for BODIPY dye with vicinal dithiol protein affinity. (**E**) (**i**) Confocal fluorescence image of selected mitochondria; (**ii**) stimulated emission depletion (STED) super-resolution image of mitochondria captured using 10% STED laser power; (**ii**, **iii**) STED super-resolution images acquired with 10% (**iii**) and 40% (**iv**) STED laser power at 592 nm, after activating the time gate to suppress background fluorescence with a lifetime of less than 0.5 ns. (**F**) Chemical structures for various mitochondria targeting BODIPY dyes reported. Reproduced with permission from [49], 2024, RSC publishing group; [58,59], ACS, 2018; [60,61], 2019, 2021, Elsevier, respectively.

Yang et al. developed a BODIPY-based fluorogenic probe that selectively binds to mitochondrial vicinal dithiol proteins (BODIPY-VDP) (Figure 7D) [58]. The probe utilizes phenylarsenicate for vicinal dithiol protein recognition and TPP+ for mitochondrial targeting. It enabled high-resolution mitochondrial imaging using varying beam strengths and time gates, revealing a distinct speckled, filamentous structure at a resolution of around 90 nm with 10% stimulated emission depletion laser power (Figure 7E). This advancement is crucial for studying vicinal dithiol proteins in mitochondrial-related diseases and diagnosing conditions linked to redox activities.

Cationic compounds can disrupt cellular function by inducing depolarization of the mitochondrial membrane, leading to unnecessary metabolic processes. To enhance the biocompatibility and cellular penetration of mitochondrial-targeted probes, Singh et al. introduced a neutral BODIPY fluorophore (BCGPEG) (Figure 7F) [59]. This innovative probe enables selective mitochondrial imaging. By incorporating small PEG chains for improved cell penetration and a CF3 group at the meso position to generate a partial positive charge, it effectively directs the probe to the mitochondria. Compared to the commonly used Mitotracker Red CMXRos, this probe exhibited superior mitochondrial selectivity, making it an invaluable tool for studying mitochondrial health. Subsequently, Gupta's team developed another neutral mitochondrial probe based on thioglycosylated BODIPYs (Figure 7F) [60]. This compound, which can also be utilized in anticancer therapies, enhances cellular uptake and exhibits significant cytotoxic effects against HeLa and HaCaT cells. Later, Yang and colleagues advanced the field with the creation of a NIR mitochondrial imaging probe (Figure 7F) [61]. This probe features piperidinyl groups as the targeting moiety, demonstrating excellent photostability, low cytotoxicity, and high membrane permeability, enabling rapid cellular uptake and targeted accumulation in mitochondria, effectively highlighting these areas.

4.4. BODIPY Dyes for Endoplasmic Reticulum Imaging

Recent studies have developed novel BODIPY derivatives that specifically target the endoplasmic reticulum (ER), improving the accuracy of imaging in live cells. For instance, the ER-Tracker Green dye, a BODIPY derivative, has demonstrated high selectivity for the ER, enabling researchers to visualize ER dynamics in living cells with high fidelity (ER-Tracker^{TM} Green (BODIPYTM FL Glibenclamide, Thermofisher). These targeted probes leverage the unique affinity of BODIPY dyes for specific cellular structures, providing insights into ER functions and stress responses, which are pivotal in understanding various diseases, such as cancer and diabetes. Several imaging techniques effectively utilize BODIPY dyes for visualizing the ER. For example, fluorescence microscopy combined with BODIPY-based dyes allows for detailed studies of ER morphology and dynamics under physiological conditions. Techniques such as fluorescence recovery after photobleaching have demonstrated how BODIPY dyes can be employed to investigate protein mobility within the ER, thereby contributing to the understanding of protein synthesis and folding. Moreover, multicolor and live-cell imaging systems, enabled by different spectrally distinct BODIPY dyes, facilitate simultaneous tracking of multiple organelles, enhancing the overall comprehension of intracellular interactions. The application of BODIPY dyes for ER imaging extends to disease research, especially concerning conditions like pancreatic ductal adenocarcinoma. For instance, a recent study by Chauhan et al. demonstrated a BODIPY-naphtholimine dyad that targets both the ER and lipid droplets within pancreatic ductal adenocarcinoma cells, showing potential for dual imaging and therapeutic applications (Figure 8A,B) [62]. This dual approach highlights the role of the ER in lipid metabolism and stress responses associated with cancer, revealing avenues for targeted therapies that exploit ER-specific pathways. Moreover, the ability of BODIPY dyes to cause

robust ER stress and cellular lipid peroxidation indicates exciting possibilities for their use in photodynamic therapy. The targeted generation of reactive oxygen species (ROS) via BODIPY dyes can selectively induce apoptosis in malignant cells (Figure 8C), suggesting a dual role not just as imaging agents but also as therapeutic tools.

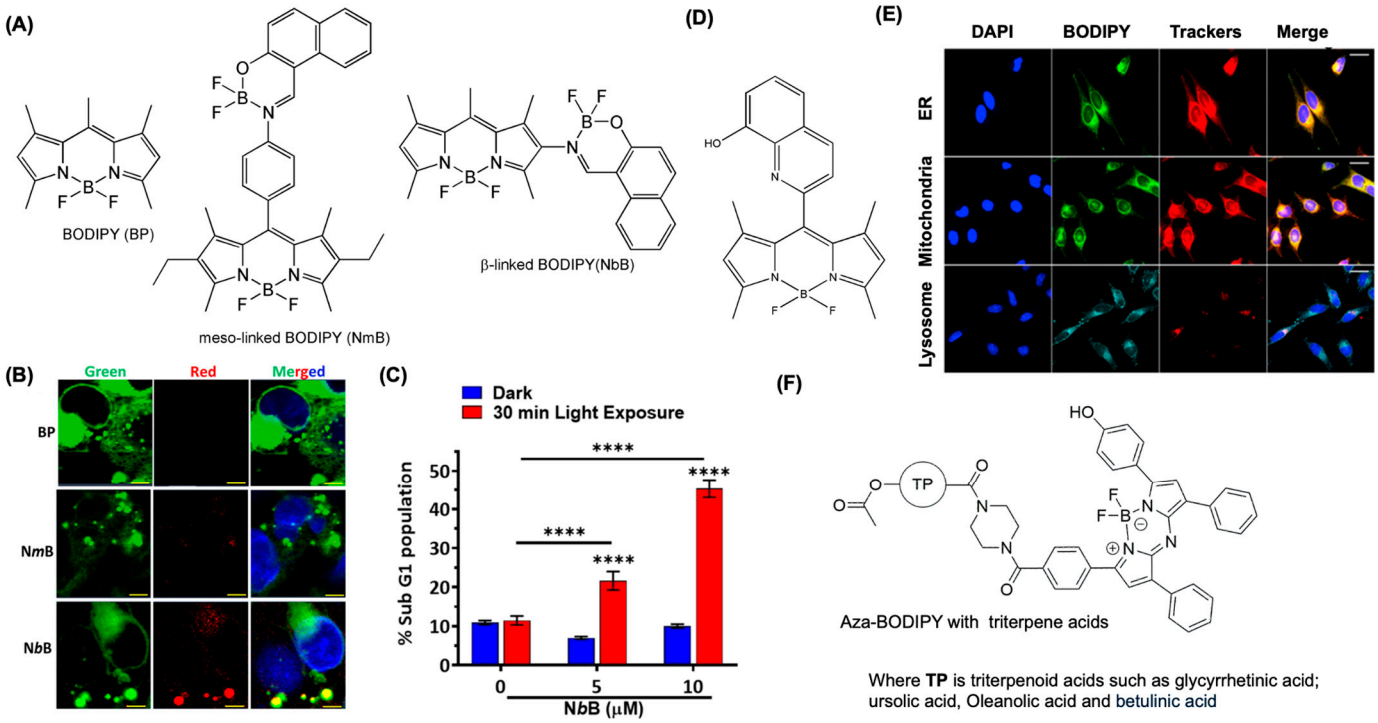


Figure 8. BODIPY dyes for endoplasmic reticulum imaging. (**A**) Chemical structure for the synthesized BODIPY dyes for ER targeting. (**B**) fluorescence microscopic images for the dye NbB localized in ER and in the lipid droplets. Scale bar = 20 μm. (**C**) Represents the PDT based response for NbB dye after 30 min of exposure with visible light after incubating them into PANC-1 cells. The % Sub G1 population shows damaged DNA and apoptosis after 24 h of exposure of the dye with visible light. (**D**) Chemical structure for the 8-hydroxyquinoline based BODIPY derivative for ER targeting and imaging applications. (**E**) Fluorescence images for the intracellular localization in HeLa cells using 8-hydroxyquniline based BODIPY dye (10 μM, excitation at 405 nm, emission collected between 420 and 480 nm) alongside ER-Tracker Red (0.2 μM, excitation at 559 nm, emission collected between 590 and 640 nm), MitoTracker Red (1 μM, excitation at 635 nm, emission collected between 640 and 690 nm), and LysoTracker Red (1 μM, excitation at 635 nm, emission collected between 640 and 690 nm). Scale bar: 30 μm. Where **** $p < 0.0001$ with respect to untreated cells. (**F**) Chemical structure for aza-BODIPY with triterpenoid acids in the backbone for ER targeting. Reproduced with permission from [62], 2024, ACS; [63], 2020, Elsevier, respectively.

Jong et al. fabricated a series of BODIPY-hydroxyquinoline derivatives for targeting ER. Among the eleven synthesized derivatives, the one with quinolin-8-ylpentanoate derivative showed enhanced localization and in vivo labeling for the ER (Figure 8D) [63]. This derivative showed a quantum yield of Φ = 55%, with low cytotoxicity, and showed more enhanced fluorescence imaging capability than the commercial ER—Tracker Red (Figure 8E).

The application of aza-BODIPY dyes in live-cell imaging has revolutionized the study of the ER. For example, real-time imaging of cellular processes such as protein folding, lipid synthesis, and stress responses can be achieved due to the persistent fluorescence of these dyes [12]. Notably, aza-BODIPY dyes can provide insights into abnormal ER dynamics in pathological conditions, including cancer and neurodegenerative diseases. By tracking the distribution of aza-BODIPY dyes within the ER in live cells, researchers can visualize alterations related to disease states and gain insights into cellular stress responses. Hoenke

et al. synthesized aza-BODIPY derivative conjugated with 3-O-acetyl-triterpene carboxylic acids using a piperazinyl spacer (Figure 8F). The fluorescence microscopy and staining experiments showed that this derivative can be used for the ER imaging of A375 cells without cytotoxicity [64].

Despite their numerous advantages, the application of BODIPY dyes in ER imaging is not without challenges. The sensitivity of BODIPY dyes to environmental factors such as pH and solvent polarity can affect their performance in live-cell imaging. There is ongoing research to improve the stability and specificity of these dyes, as well as to expand their compatibility with various imaging modalities. Future studies may focus on synthesizing next-generation BODIPY derivatives with enhanced properties for more precise and robust imaging applications.

4.5. BODIPY Dyes for SERS-Based Bioimaging

Surface-Enhanced Raman Scattering (SERS) is a spectroscopic technique that significantly increases the intensity of Raman scattering of molecules adsorbed on nanostructured metallic surfaces, typically gold or silver. This enhancement is achieved through two primary mechanisms: the electromagnetic effect, which arises from localized surface plasmons that amplify the incident light field, and the chemical effect, which involves changes in the molecular polarizability due to interactions with the metallic substrate. The combination of these effects allows SERS to achieve high sensitivity, enabling the detection of single molecules and providing detailed information about their chemical structures [65,66]. Raman spectroscopy of BODIPY molecules reveals characteristic peaks related to specific vibrational modes, including C-H stretching (around 2965, 2925, and 2850 cm^{-1}), C=C (around 1652.72 and 1593.83 cm^{-1}), B-N and C-N moieties (around 1590 and 1208.42 cm^{-1}), which can be enhanced when functionalized BODIPY can interact with Au or Ag NPs. When combined with SERS, BODIPY dyes serve as effective Raman reporters, enhancing signal detection through the electromagnetic field produced by metallic nanostructures [67]. This enhancement is pivotal because it allows for the detection of biomolecules at lower concentrations than would be possible with traditional fluorescence techniques. The high specificity of BODIPY dyes for targeted biological molecules, combined with the sensitivity of SERS, positions them as valuable tools in bioimaging applications, particularly in the context of health diagnostics and monitoring disease progression.

Adarsh et al. fabricated a series of aza-BODIPY derivatives (1–6), which can adsorb on AuNPs surface for enhanced SERS response for these dyes (Figure 9A,B) [68]. Among the series of aza-BODIPY dyes, the derivative 4 showed excellent photophysics in terms of stability, and Raman response under excitation using a laser. Remarkably, it identified three human cancer cell types (A549, HeLa, and HT-1080) without requiring specific surface markers, producing clear Raman mapping and signature peaks (Figure 9C). A cluster analysis was conducted using characteristic Raman spectral scans for each cancer cell line, under the assumption that the Raman nanotag was likely localized near the cell surface. This proximity of 4-Au@PEG to the cell surface was further validated through three-dimensional Raman imaging and single spectral analysis, which revealed distinctive SERS peaks corresponding to the aza-BODIPY probe 4-Au@PEG. However, no such recognition occurred in normal fibroblast (3T3L1) cells. To validate, the nanoprobe was conjugated with EGFR, a tumor-targeting marker for HT-1080 cells. This enhanced the probe's specificity for cancer cells, enabling ultrasensitive detection and targeted imaging while sparing normal cells (Figure 9D). Klapper et al. showed that using Raman spectroscopy the proportions of body fat and fat-free mass can be identified and imaged for metabolic *C. elegans* [69]. As shown in Figure 9C, BODIPY 493/503-labeled structures overlapped with lipid signals as measured by Raman spectroscopic measurements.

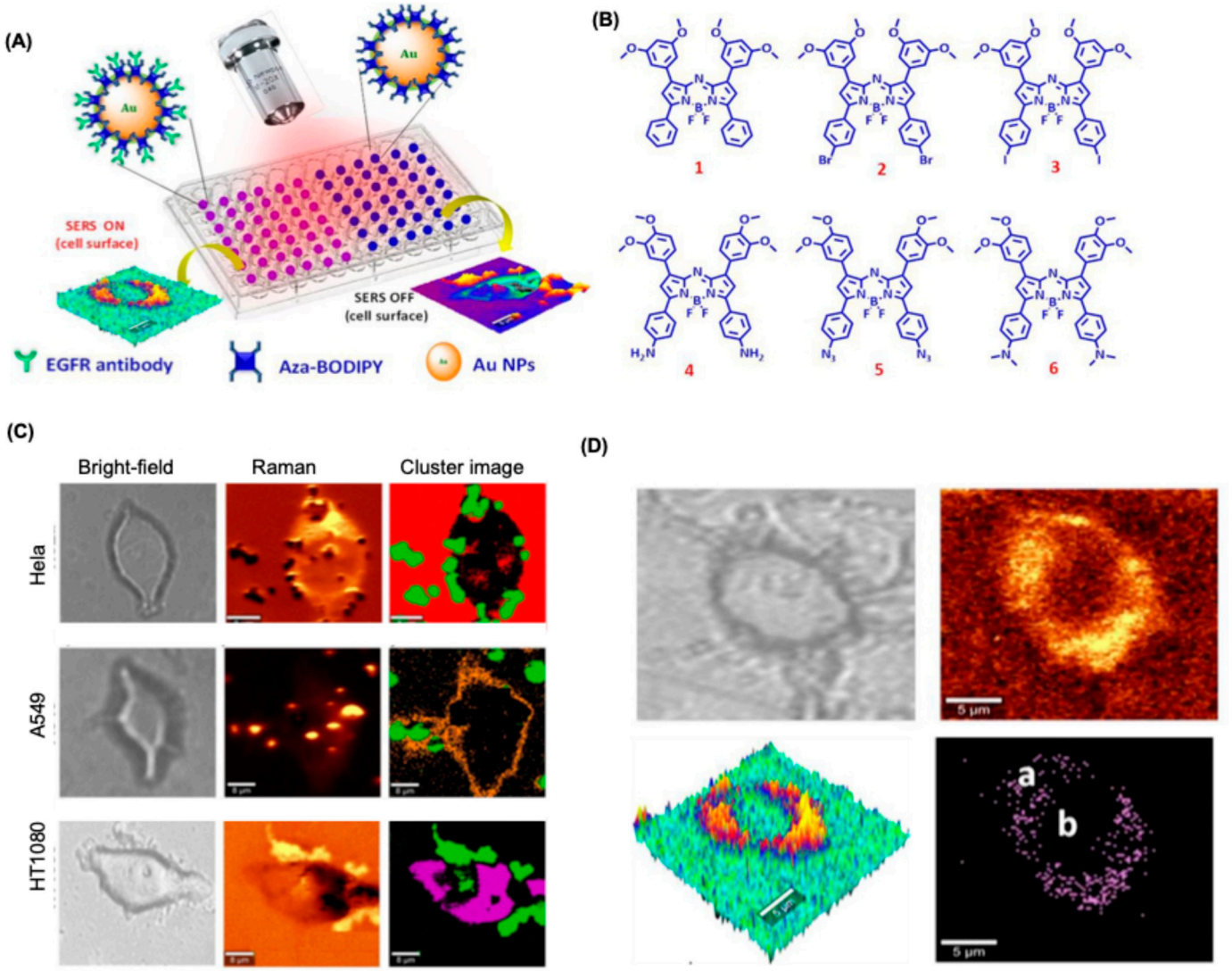


Figure 9. BODIPY dyes for Raman based imaging. (**A**) A schematic for the working principle of aza-BODIPY dye for SERS based Raman imaging in tumor cells. (**B**) Chemical structures for a series of aza-BODIPY dyes for Raman based imaging applications. (**C**) Bright field, Raman and Cluster images for the aza-BODIPY dye 4 conjugated with Au and PEG for Raman mapping studies in three different cancer cells. Scale bar 8 μm. (**D**) Bright field, Raman, 3D color code Raman and Cluster images for aza-BODIPY dye 4-PEG with targeting group EGFR incubated with HT1080 cell line, where (**a**) single spectra abstracted from the cluster mapped region, and (**b**) in the cluster mapped image. Reproduced with permission from [68], 2017, Wiley.

4.6. BODIPY Dyes for Photoacoustic-Based Bioimaging

Photoacoustic imaging (PAI) is an advanced biomedical technique combining optical imaging and ultrasound. It uses the photoacoustic effect, where absorbed light converts to ultrasound signals, enabling high-resolution tissue imaging [70–72]. While PAI relies on endogenous chromophores like hemoglobin, exogenous contrast agents enhance imaging capabilities. These agents, including organic dyes (e.g., indocyanine green) and nanoparticles (e.g., gold), optimize light absorption in the near-infrared spectrum for deeper penetration and improved contrast. Novel materials, like semiconducting polymers and metallic nanoparticles, further enhance specificity and signal intensity, particularly for cancer diagnostics in complex tissue environments.

The BODIPY chromophores have been widely used in bioimaging, yet they are not ideal for PAI due to high fluorescence. But with the advancements in synthesis and tuning

their optical properties, BODIPY dyes have recently been used for PAI applications [73–75]. For instance, modifications such as 1H-pyrrole conjugation can lead to increased absorption wavelengths, extending up to 799 nm, which is advantageous for PAI [76]. A nonfluorescent PyBODIPY dye series was designed through 1H-pyrrole conjugation, and enabled PA signal detection at low concentrations, with a sensitivity reaching 1 nmol/mL in tubes and 35 pmol/mm^3 in tissue phantoms (Figure 10A,B). In addition to being nonfluorescent, they are non-phototoxic, photostable, and exhibit high molar extinction coefficients and resistance to nucleophilic addition. PEG-400 modification enhances their aqueous solubility, making them suitable for in vivo imaging. PyBODIPY's properties make it a promising PA contrast agent, with the potential for coupling to targeting ligands and further applications in designing near-infrared quenchers for clinical translation. Ni et al. prepared a naphthalene fused BODIPY dimer Na-BD which possesses excellent photostability and NIR absorption band between 600 and 850 nm (Figure 10C) [73]. On evaluation of their PA imaging capability, the BODIPY dimer showed excellent PAI signals compared to commercial indocyanine green dye. Na-BD was further loaded into bovine serum albumin nanoparticles and was injected into mice having the Hep-G2-tumor. The PAI imaging studies showed the accumulation of these formulations inside the tumor region, with a sharp contrasting effect to indocyanine green (Figure 10D). Similar studies were performed using a meso-ester substituted BODIPY near-infrared dyes for the PAI applications for Hep-G2-tumor-bearing mice [74]. Enhanced PA signals were observed for 72 h of post injection. Ma et al. reported an aza-BODIPY derivative for monitoring the variation of $ONOO^-$ ions in vivo using PAI [77]. The PA signal can be controlled by the ICT effect and by the electron-withdrawing group at 2-posiiton of BODIPY dye. This can be used for studying arthritis inflammation in mice, and as shown in Figure 10E, the left limb injected with λ-carrageenan showed a PA signal three times more intense than the right limb which was injected with saline. Arthritis causes an increased elevation in the level of $ONOO^-$ ions, thus resulting in a lesser PA signal from the left limb. In another study, a ratiometric signal probe was used for monitoring the oxidative stress, and activated neutrophils in plaques [78]. A BODIPY core attached with neutrophil elastase peptide was fabricated, and under oxidative stress the peptide cleaves enhance the photoinduced electron transfer impacting photoacoustic intensity at 685 and 745 nm as studied by in vivo experiments.

A donor-acceptor derivative was fabricated by Xu et al. (Figure 10F) [79]. The designed BODIPY dye showed absorption within 700–1000 nm with excellent photostability and photoacoustic signal properties depending on the functional groups. Among the series, the BODIPY dyes such as BX9 and BX11 showed PA signal intensity with a distinguishable signal even at a depth of 4 mm using chicken breast and showed a clear distinguishable signal from the ultrasound signals. In vivo experiments showed the BODIPY dye can accumulate in both venous vessels and intestines, thereby dissecting the relevant physiological or pathological events of these two organs (Figure 10G).

Thus, the adoption of BODIPY dyes in photoacoustic imaging represents a significant advancement in biomedical diagnostics. Their distinct optical properties, ease of modification, and broad applicability in various medical fields underline their potential as invaluable tools in improving patient care and outcomes in the realm of medical imaging.

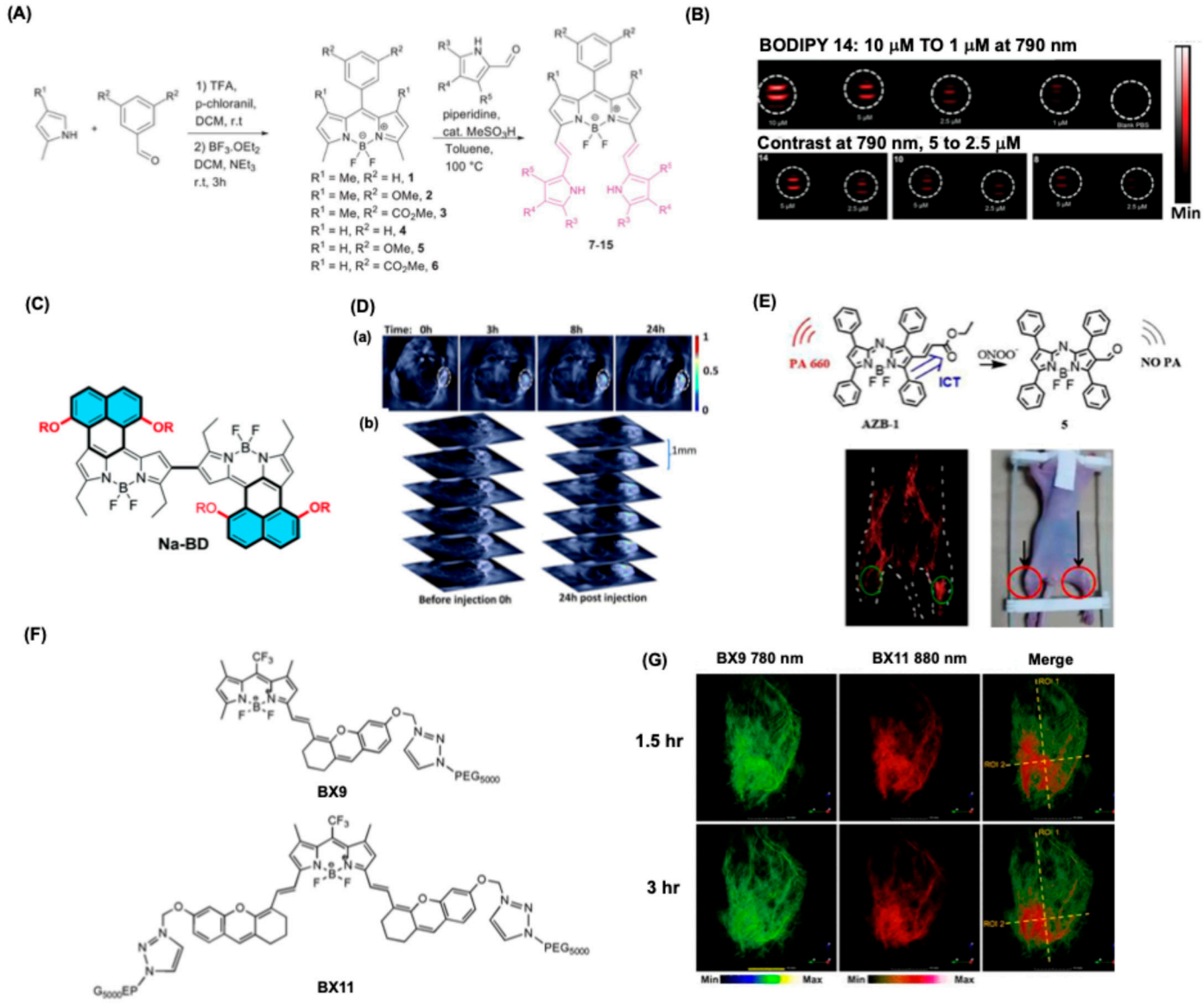


Figure 10. BODIPY dyes for photoacoustic imaging. (**A**) Synthetic route for Py-BODIPY dyes for PAI applications. (**B**) PA image snapshot at 790 nm of py-BODIPY 14 in PBS with dilution of 10×10^{-6} to 1×10^{-6} M and the PA image snapshot at 790 nm of py-BODIPY (14, 10, 8) at 5 and 2.5×10^{-6} M in PBS. (**C**) Chemical structure, and (**D**) time dependent in vivo PAI for a Hep-G2-tumor bearing mouse injected with Na-BD 2.5 wt% (**a**) and (**b**) three-dimensional rendering of the scanning area before injection and 24 h post injection (the images were zoomed in to make the tumor site clearer). Circles indicate the tumor region. (**E**) Working principle and in vivo PAI for arthritis mice after injecting BODIPY dye which is responsive for PAI after $ONOO^-$ sensing. AZB-1 initially exhibited a strong photoacoustic signal at 660 nm. However, the addition of $ONOO^-$ suppressed its PA signal by inhibiting the ICT effect. Furthermore, the probe was effectively utilized to monitor $ONOO^-$ fluctuations in mouse models of inflammation. Circles showing the arthritis region in the mice. (**F**) Chemical structures for xanthene appended BODIPY derivatives BX9 and BX11. (**G**) Two-channel 3D PA images of the 780 nm channel with BX9 for the vasculature and the 880 nm channel with BX11 for the intestine, respectively, at two different time points. Scale bar: 10 mm. Reproduced with permission from [76], 202, Wiley; [73], 2016, RSC publishing group; [77], 2021, Elsevier Publishers; [79], 2024, ACS, respectively.

5. Therapeutical Application of BODIPY

5.1. BODIPY Dyes in Photodynamic Therapy (PDT)

Photodynamic therapy (PDT) is widely used in cancer treatment, relying on a photosensitizer (PS), light, and oxygen. Upon light activation, the PS enters an excited state and returns to the ground state by emitting fluorescence or generating heat which can be explained by Jablonsky diagram as shown in Figure 11A [80–82]. It can also undergo intersystem crossing, forming a triplet state (^{3}PS*), which interacts with oxygen to produce singlet oxygen ($^1O_2$) in Type II reactions or reactive oxygen species (ROS) in Type I reactions. These ROS drive cell death through necrosis, apoptosis, and autophagy while triggering immune responses (Figure 11B). An ideal PS should selectively target tumors, balancing lipophilicity for uptake and hydrophilicity for administration. It must be non-toxic to healthy cells, chemically stable, and efficiently generate singlet oxygen. Optimal activation occurs in the 680–800 nm range for deeper tissue penetration.

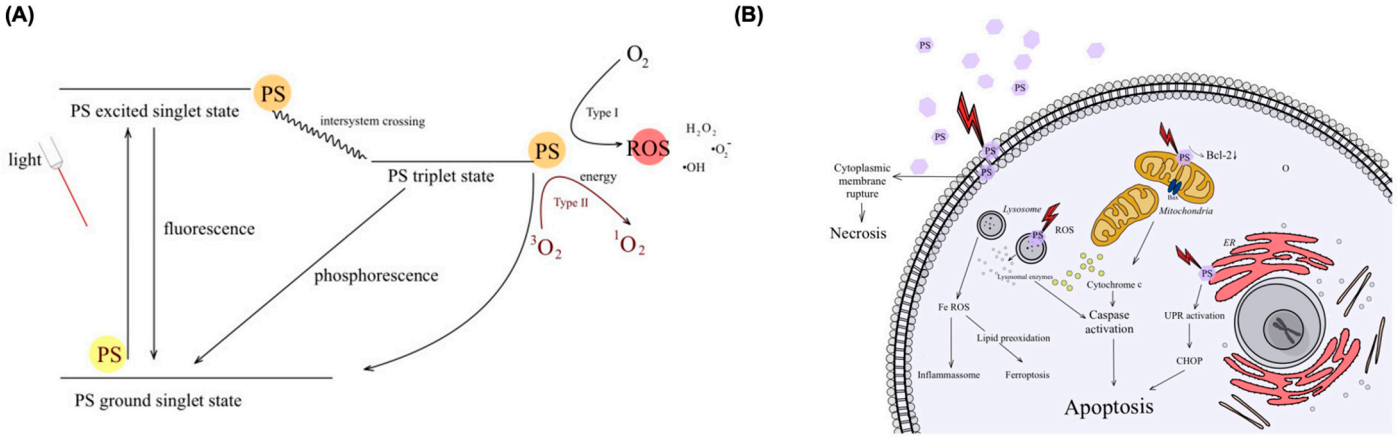


Figure 11. (**A**) Jablonski diagram showing photophysical processes occurring during PDT. (**B**) Schematic representation of cancer cell death by apoptosis and necrosis after PDT activation. Reproduced with permission from [82], 2023, MDPI publishers.

BODIPY dyes, widely recognized for their exceptional biomarker capabilities, have evolved into crucial tools for photodynamic therapy (PDT) when strategically designed. Photodynamic therapy employs a combination of light, a photosensitizing agent, and molecular oxygen to target and eliminate abnormal cells, particularly cancerous ones. Recently, a novel generation of PDT agents rooted in the BODIPY core has emerged, showcasing significant potential in therapeutic applications over the past decade [81,83]. The incorporation of heavy atoms, such as halogens and metal ions, into the BODIPY framework serves as a fundamental strategy to enhance its photosensitizing attributes. This deliberate arrangement of heavy atoms such as iodine, bromine, and metal ions within the BODIPY structure promotes spin-orbit coupling (SOC), facilitating intersystem crossing (ISC). These processes are critical to the increased production of reactive oxygen species (ROS), which act as mediators of cell destruction through various programmed cell death pathways. Consequently, the tailored design of BODIPYs as photosensitizers marks a significant advancement in the efficacy of photodynamic therapy for cancer treatment. A list of various BODIPY dyes used for PDT applications is represented in Figure 12.

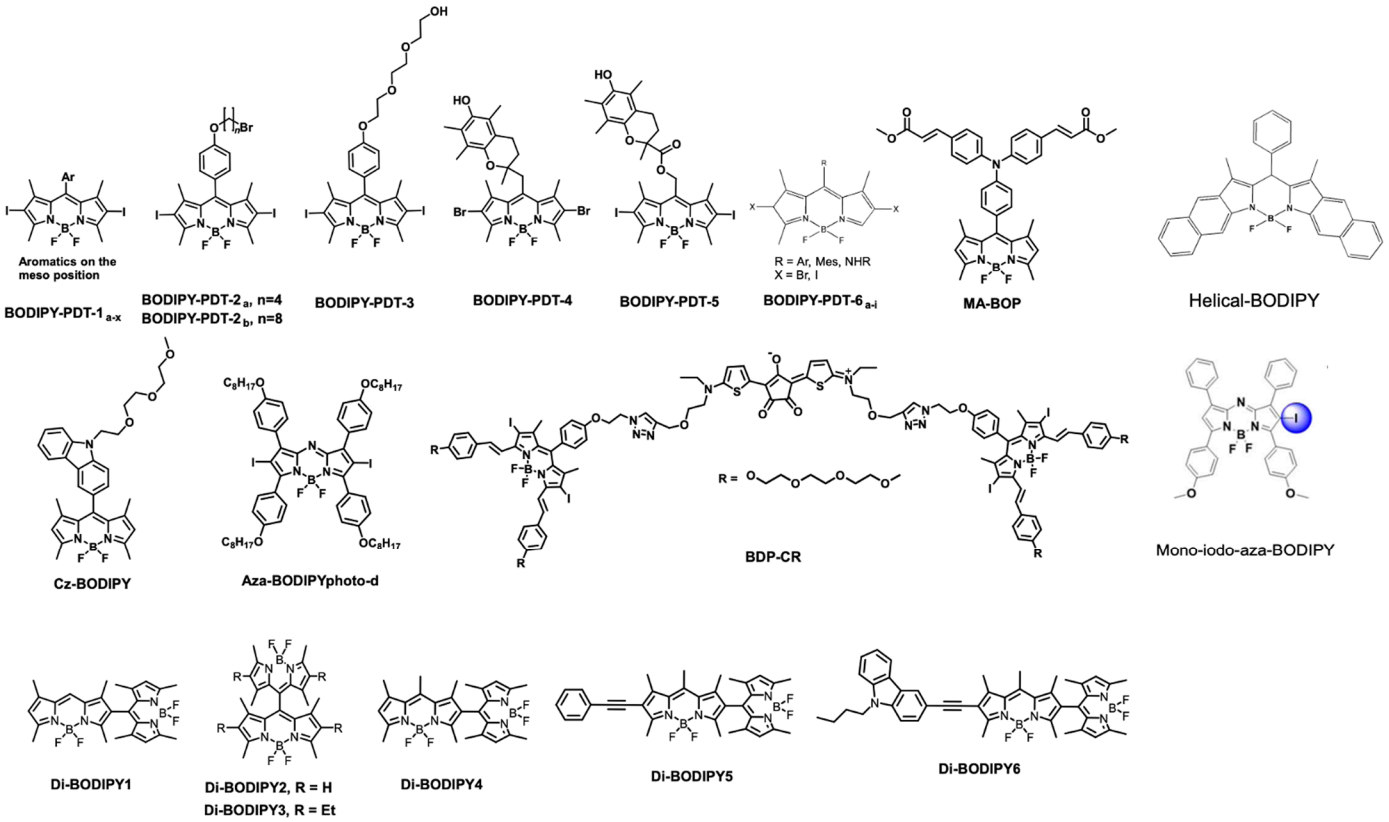


Figure 12. List of BODIPY and aza-BODIPY dyes used for PDT based applications.

For instance, Caruso et al. investigated the photodynamic therapeutical effectiveness of various BODIPYs, specifically the BODIPY-PDT-1a-x and BODIPY-PDT-2a-b compounds. They incorporated an aromatic ring in the meso position along with iodine atoms located in the β-positions, which demonstrated enhanced efficiencies in singlet oxygen production [84,85]. Similarly, Kim et al. focused on a BODIPY variant known as BODIPY-PDT-3, which displayed remarkable singlet oxygen sensitization capabilities, effectively inducing necrosis in Lewis lung carcinoma cells during in vitro analyses [86].

In addition, Cosa and colleagues showcased ROS's role in activating singlet oxygen photosensitizers [87]. They found that the inclusion of a trap segment in BODIPY-PDT-4 enhanced its control over singlet oxygen sensitization compared to BODIPY-PDT-5, thereby presenting a substantial improvement in the management of photodynamic reactions. Further investigations by Epelde-Elezcano et al. highlighted the differences in singlet oxygen generation between halogenated BODIPY dyes, illustrating that iodine atoms enhanced ISC more effectively than bromine atoms in the variant BODIPY-PDT-6a-I [88].

Moreover, Zhao and their teams successfully synthesized a near-infrared (NIR) monoiodinated aza-BODIPY photosensitizer, which exhibited significant efficacy in vivo for photodynamic applications [89]. Yoon et al. contributed by developing highly efficient triplet BODIPY derivatives aimed at photodynamic treatment and bioimaging roles [90]. Recent advancements also include the work by Qian et al., who reported the development of orthogonally linked donor-acceptor-framed BODIPY variants, such as MA-BOP and Cz-BODIPY, which induced ISC providing promising avenues for intracellular photodynamic therapy [91,92]. Furthermore, Wang et al. made strides by introducing a heavy-atom-free helical BODIPY derivative that demonstrated a record low dosage effectiveness in PDT-augmented immunotherapy [93].

BODIPY dimers with intersystem crossing have emerged as promising triplet photosensitizers for PDT, photocatalysis, and photon up conversion. These dimers, formed by

linking two BODIPY molecules, must exhibit stable absorption/emission wavelengths and efficient ROS generation. Cakmak et al. reported orthogonal BODIPY dimers (Di-BODIPY1–3) with singlet oxygen quantum yields of 51%, 46%, and 21%, respectively, confirming their phototoxicity in cancer cells [94]. Wu et al. synthesized Di-BODIPY4–6 to extend absorption wavelengths, with fluorescence quantum yields of 2.2%, 17.6%, and 2.3% [95]. The triplet state lifetimes of Di-BODIPY4 and Di-BODIPY5 were 115.6 and 140.9 µs.

The extensive literature now includes systematic reviews addressing the applications and advancements of heavy-atom-free BODIPY-based photosensitizers in photodynamic therapy, emphasizing their growing significance in therapeutic contexts [80,96–98]. The application of various BODIPY derivatives for PDT applications are summarized in Table 1.

Table 1. Application of various BODIPY derivatives for PDT application.

Theranostics	Photophysics	Light Source	Therapeutic Modalities	In Vitro/In Vivo Tumor	Ref.
BODIPY-PDT-1a-x	Φ_{fluo} = 0.01 to 0.04 $^1O_2$ = 0.90 to 2.67	Green LED fluence: 25.2 J/cm^2	PDT	SKOV 3 cells,	[85]
BODIPY-PDT-2a, n = 4	Φ_{fluo} = 0.01 $^1O_2$ = 1.10	Green LED	PDT	HCT116, SKOV3 and MCF7	[84]
BODIPY-PDT-2b, n = 8	Φ_{fluo} = 0.01 $^1O_2$ = 1.11	Green LED	PDT	HCT116, SKOV3 and MCF7	[86]
BODIPY-PDT-3	Φ_{fluo} = 0.02 $^1O_2$ = 0.93	Hg light; 0.2 mW/cm^2	PDT	LLC cells	[87]
BODIPY-PDT-4	Φ_{fluo} = 0.008 $^1O_2$ = 0.80	Nd: YAG laser; 2.6 mW/cm^2	PDT	Gram negative E. coli strain	[87]
BODIPY-PDT-5	Φ_{fluo} = 0.009 $^1O_2$ = 0.57	Nd: YAG laser; 2.6 mW/cm^2	PDT	Gram negative E. coli strain	[87]
BODIPY-PDT-6a-i	Φ_{fluo} = 0.01 to 0.51 $^1O_2$ = 0.09 to 0.96	xenon flash lamp; 450 W	PDT	Not performed	[88]
MA-BOP	Φ_{fluo} = 0.56 $^1O_2$ = 0.2	monochrome light; 12 W	PDT	A-549 cells	[91]
Cz-BODIPY	Φ_{fluo} = 0.10 $^1O_2$ = 0.68	White light; 4 mW cm^{-2}	PDT/FL	Bel-7402 cells and Zebra fish	[92]
Mono-iodo-aza-BODIPY	Φ_{fluo} = 0.08 $^1O_2$ = 0.52	75 W halogen lampi; 54 J/cm^2 for in vitro. 90 mW/cm^2 for in vivo	PDT	HeLa, (MCF-7), SW480; HeLa tumor-bearing nude mice	[89]
Helical BODIPY	Φ_{fluo} = 0.21 $^1O_2$ = 0.36	Irradiation by 656 nm LED, light dose: 6 J cm^{-2}	PDT augmented checkpoint blockade immunotherapy	CT26 tumor cells and CT26 tumors on BALB/c mice	[93]
Di-BODIPY 1–3	Φ_{fluo} = 0.03, 0.31, 0.49, respectively $^1O_2$ = 0.51, 0.46, 0.21, respectively. Di-BODIPY 6 showed a lower value for detection	LEDarrayat 2.5 mW cm^{-2}	PDT	K562	[97]
Di-BODIPY 4–6	Φ_{fluo} = 0.02, 0.17, 0.023, respectively $^1O_2$ = 0.64, 0.42, respectively. Di-BODIPY 6 showed a lower value for detection	Spectrofluorometer light	Not performed	Not performed	[95]

5.2. BODIPY Dyes in Photothermal Therapy (PTT)

The primary mechanism of PTT involves the selective heating of tumor cells through the photothermal effect [99,100]. When light, particularly near-infrared (NIR) light, is delivered to tumor sites, it is absorbed by photothermal agents, which can include nanoparticles and organic dyes that possess strong light absorption properties. These agents convert the absorbed light into heat, leading to localized hyperthermia that can induce apoptosis, necrosis, or a combination of both in cancer cells. The temperature increase can exceed 50 °C, which is sufficient to disrupt cellular components and induce cellular death. In addition to direct tumor destruction, PTT can also stimulate an immune response against the tumor. The heat generated during the process can cause immunogenic cell death, leading to the release of tumor antigens and promoting the activation of immune cells, which can further enhance the anti-tumor effect. Thus, PTT not only acts directly on cancer cells by causing thermal damage but also indirectly by enhancing the body's immune response against the tumor.

BODIPY dyes possess remarkable photothermal conversion efficiencies, particularly in the near-NIR region, which is advantageous for penetrating biological tissues with minimal damage. Their tunable absorption properties allow for precise customization based on the specific wavelengths required for effective PTT. PTT kills cancer cells by hyperthermia or by generation of heat-shock proteins. BODIPY dyes exhibit strong absorption in the NIR range, making them suitable candidates for applications where deeper tissue penetration is needed. For instance, researchers have developed π-extended BODIPY dyes that achieve over 90% photothermal conversion efficiency, highlighting their effectiveness in converting light energy into heat (Figure 13A) [32]. Upon 808 nm laser irradiation (0.75 W cm^{-2}), the temperature of aqueous dispersions of the meso-CF_3-BODIPY NPs (20 μm based on dye) increased with time and reached a maximum at 66.8 °C (ΔT = 43 °C, TCF_3PEn), 64.9 °C (ΔT = 41 °C, TCF_3MEn), and 64.3 °C (ΔT = 41 °C, DCF3MEn) within 5 min (Figure 13B). The in vitro and in vivo studies showed an enhanced tumor ablation using a MCF-7 Xenograft model with a 50% reduction in tumor volume after the treatment.

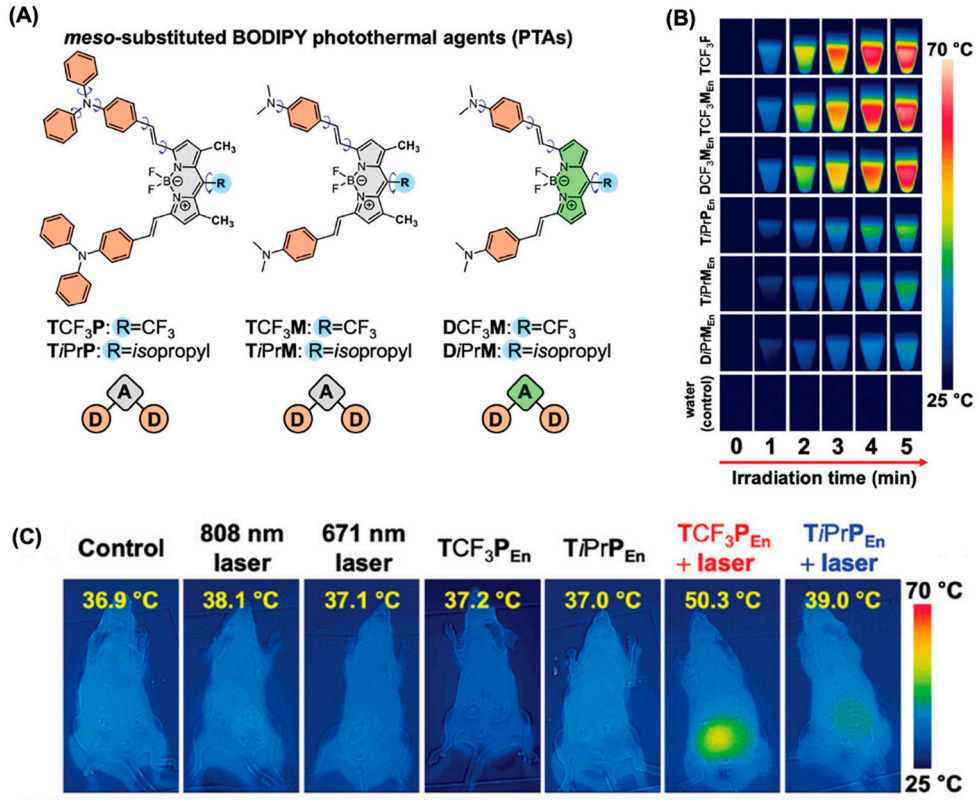


Figure 13. BODIPY dyes for PTT application. (**A**) Chemical structure for a series of BODIPY dyes. (**B**) IR thermal images for the synthesized BODIPY dyes under 808 nm laser irradiation (0.75 W cm^{-2}). TCF_3MEn and TCF_3PEn showed a rise in temperature. (**C**) Thermal infrared images illustrating temperature variations at tumor sites in mice following intratumoral injection, either with or without (TCF_3PEn or TiPrPEn, 15 μM, incubated for 2 h), and subsequent laser irradiation (0.3 W cm^{-2} for 5 min). Reproduced with permission from [32], 2024, Wiley.

As shown in Figure 13C, the meso-CF_3 substituted BODIPY (TCF_3M) showed exceptional efficacy in inducing cancer cell apoptosis and in vivo tumor ablation using low-power NIR laser irradiation (0.3 W cm^{-2}, 808 nm) compared to the other derivatives studied. In another study, Li et al. showed a series of aza-BODIPY derivatives can be used for PTT applications with a photothermal conversion efficiency of 48–50% with an anticancer property towards human colon cancer cells [101].

Liu et al. fabricated an aza-BODIPY derivative with a strong NIR absorption at 781 nm having excellent photostability and PT conversion efficiency (Figure 14A) [102]. PT studied

showed the photothermal effect is concentration dependent and a maximum temperature of 74.5 °C was attained for a concentration of 35 μg mL^{-1} upon irradiation for 5 min. As shown in Figure 14B, a dose-dependent cell cytotoxicity was observed for the dye after laser irradiation for CT26 cells. The in vivo imaging and simultaneous PTT showed a maximum temperature rise of 44.9 °C after 1 min of irradiation with a suppression in tumor of about 96 % for intertumoral injection and 89 % for intravenous injection (Figure 14C). The body weight of the mice increased within days indicating no significant toxic effects after PTT. In a similar work, Pewklang et al. showed that aza-BODIPY-Pyrazole derivative can show excellent NIR absorption at 900 nm with photothermal conversion efficiency up to 33 % (Figure 14D) [103]. The confocal microscopic images showed that these dyes can penetrate the cancer cells less than in 6 h, and PTT studies showed the elimination of 70% of cancer cells. Moreover, the same dye was used for antibacterial studies towards Escherichia coli 780, and Staphylococcus aureus 1466 with 100 % activity upon laser irradiation (Figure 14E).

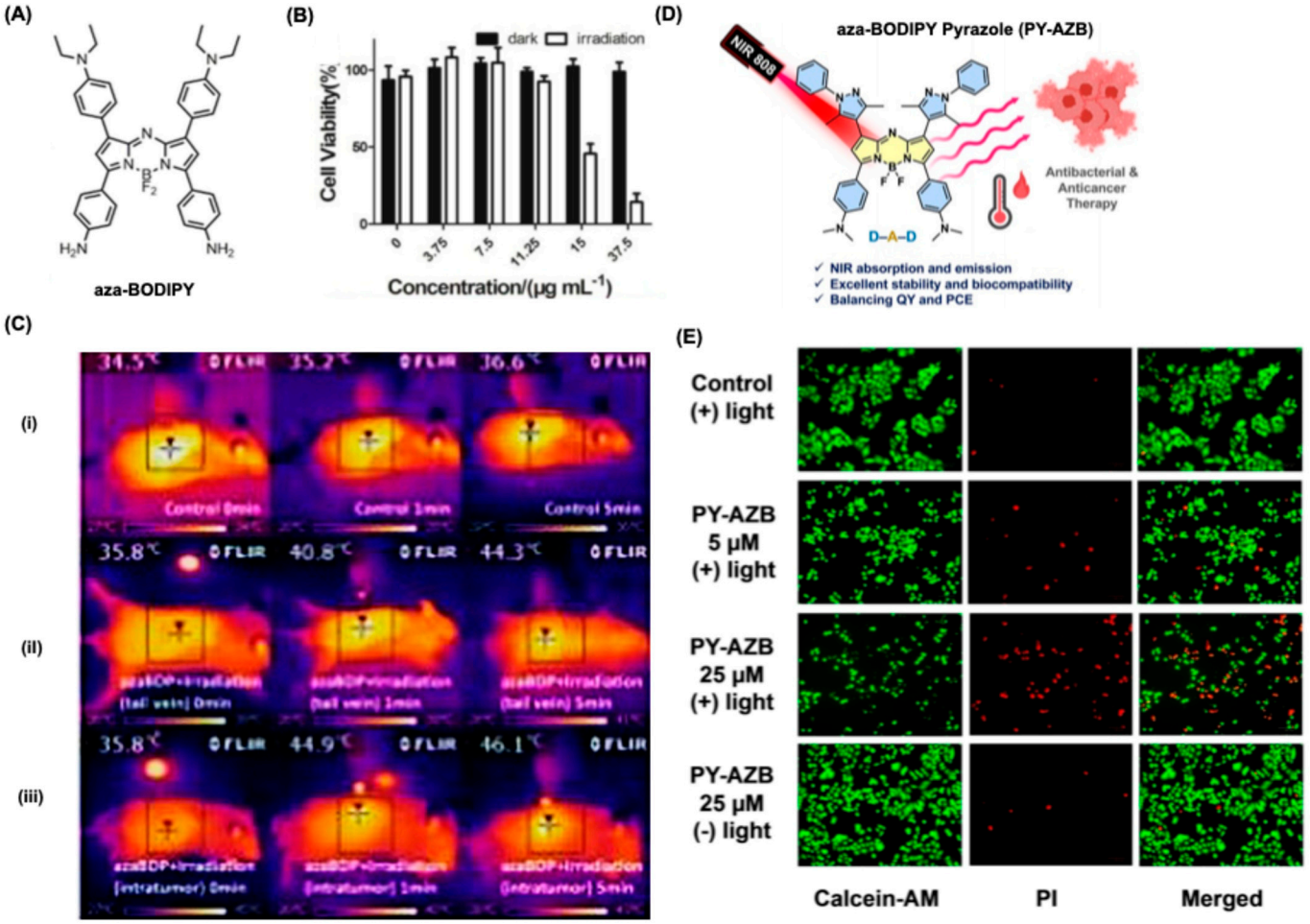


Figure 14. (**A**) Chemical structure for aza-BODIPY for PTT application. (**B**) Concentration dependent phototoxicity for aza-BODIPY derivative with CT26 cell lines (1 W cm^{-2} for 5 min). (**C**) In vivo PTT study: the whole-body thermal images of (**i**) control, (**ii**) injected tail vein, and (**iii**) injected intratumor of azaBDP solution (0.1 mL, 2 mg mL^{-1}, dissolved by Vcaster oil:Vethanol: VPBS = 1:1:2). (**D**) Chemical structure and working principle for aza-bodipy-pyrazole derivative for PTT application. (**E**) Confocal microscopic images for tumor cells treated with aza-BODIPY-Pyrazole with various treatment conditions. Reproduced with permission from [102,103], 2018 and 2024, Wiley publishing group.

The application of BODIPY dyes in photothermal therapy highlights their potential as transformative agents in oncological treatments. Their favorable photophysical properties, coupled with the ability to serve multifunctional roles, enable BODIPY dyes to offer targeted

and effective thermal ablation of tumors. As research progresses, the incorporation of these dyes into combined therapies may further enhance cancer treatment modalities, paving the way for innovative solutions that address the complexities of cancer management. Continued exploration of BODIPY dyes will undoubtedly solidify their role as critical components in the evolving landscape of photothermal therapy and cancer treatment strategies.

5.3. BODIPY Dyes in Boron Neutron Capture Therapy (BNCT)

Boron Neutron Capture Therapy (BNCT) represents a pioneering strategy in cancer treatment that leverages the unique properties of boron-containing compounds and neutron irradiation to selectively target and destroy tumor cells [104,105]. BNCT operates based on the nuclear capture of low-energy thermal neutrons by stable boron-10 atoms, which leads to a high-energy reaction. Once sufficient boron is localized in the tumor, the patient is exposed to a neutron beam, resulting in the emission of high-linear energy transfer (LET) alpha particles and lithium-7 ions ($^{10}B_5 + {}^1n_0(th) \rightarrow [{}^{11}B_5]^* \rightarrow {}^4He_2\ (\alpha) + {}^7Li_3 + 2.38$ MeV). These particles, such as alpha particles, provide high energy along their very brief pathway (<10 μm). Hence, their energy deposition is limited to the diameter of a single cell. Thus, only neoplastic cells with 10B are ravaged following thermal neutron irradiation which damages the DNA in tumor cells. Hypothetically, any normal cells abutting the cancer cells are saved from high LET irradiation by ^{4}He and ^{7}Li particles (Figure 15).

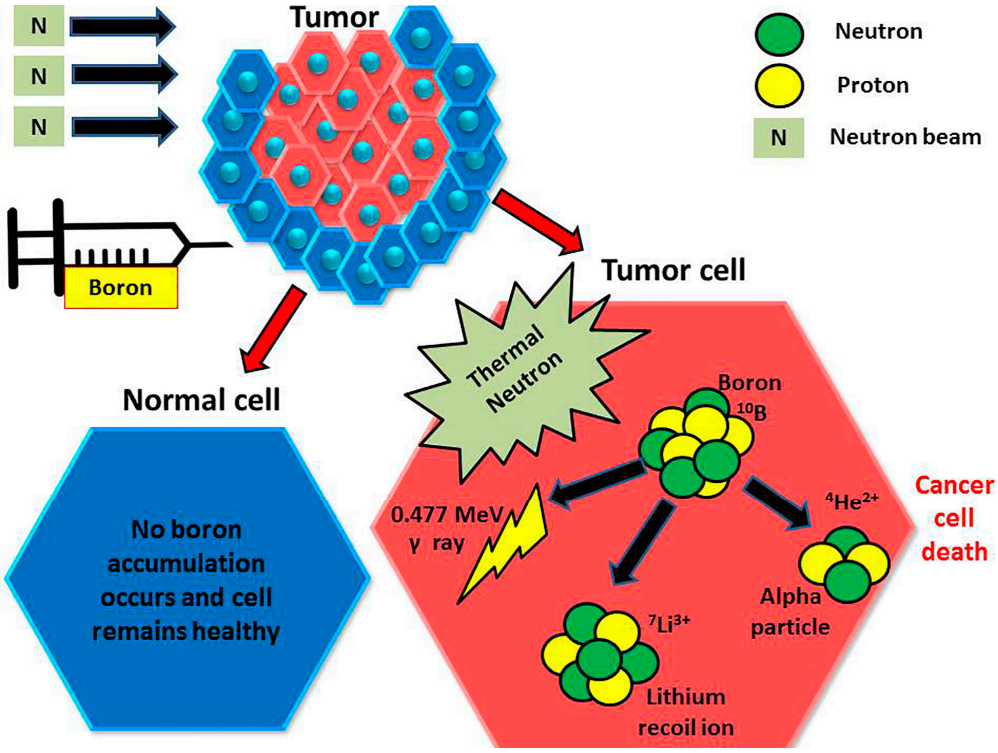


Figure 15. Working principle for BNCT. Reproduced with permission from [106], 2021, Frontiers.

Among the emerging boron carriers, BODIPY derivatives have shown significant promise due to their favorable characteristics, including high photostability, biocompatibility, and the ability to accumulate preferentially in tumor tissues. BNCT relies on the interaction between stable boron-10 isotopes (^{10}B) and low-energy thermal neutrons to induce a nuclear reaction that produces high-linear energy transfer particles, specifically alpha particles and lithium-7 ions. These particles are cytotoxic and can kill cancer cells within a subcellular range of about 10 μm. The effectiveness of BNCT is contingent upon achieving a sufficiently high concentration of boron in tumor tissues while minimizing

accumulation in surrounding healthy tissues [105,107]. Recent studies have indicated that BODIPYs can serve as efficient boron delivery vectors as they demonstrate a significant uptake in tumor cells and maintain high tumor-to-normal tissue ratios, making them suitable candidates for BNCT applications [108,109].

BCNT shows promising results for glioblastoma treatment, but the major difficulty for this treatment is the passage of drug/boron through the blood–brain barrier (BBR). To address this challenge, researchers are investigating innovative solutions to enhance boron delivery to tumor sites. Among these solutions, carborane-BODIPY derivatives have been synthesized as potential agents for BNCT. Specifically, studies conducted by M.G. Vicente et al. focused on assessing the permeability of these derivatives, BDP-Me-oCB-20 and BDP-Me-oCB-21, using human brain endothelial cell lines, such as hCMEC/D3 (Figure 16A(i,ii)) [108,110]. Their findings revealed that BDP-Me-oCB-20 exhibited a permeability coefficient (Pe) of 0.05 $\times$ 10^{-6} cm/s, while BDP-Me-oCB-21 demonstrated a Pe of 0.13 $\times$ 10^{-6} cm/s, indicating that both derivatives were inadequately internalized. The poor uptake is likely attributed to their high hydrophobicity, as evidenced by their log *p* values of 1.41 and 1.35, respectively. Consequently, enhancing the properties of carborane-BODIPY derivatives to improve their BBB penetration remains crucial for their application in BNCT. Continued research in optimizing these compounds is anticipated, aiming to increase their therapeutic efficacy against GBM while mitigating the limitations imposed by the BBB.

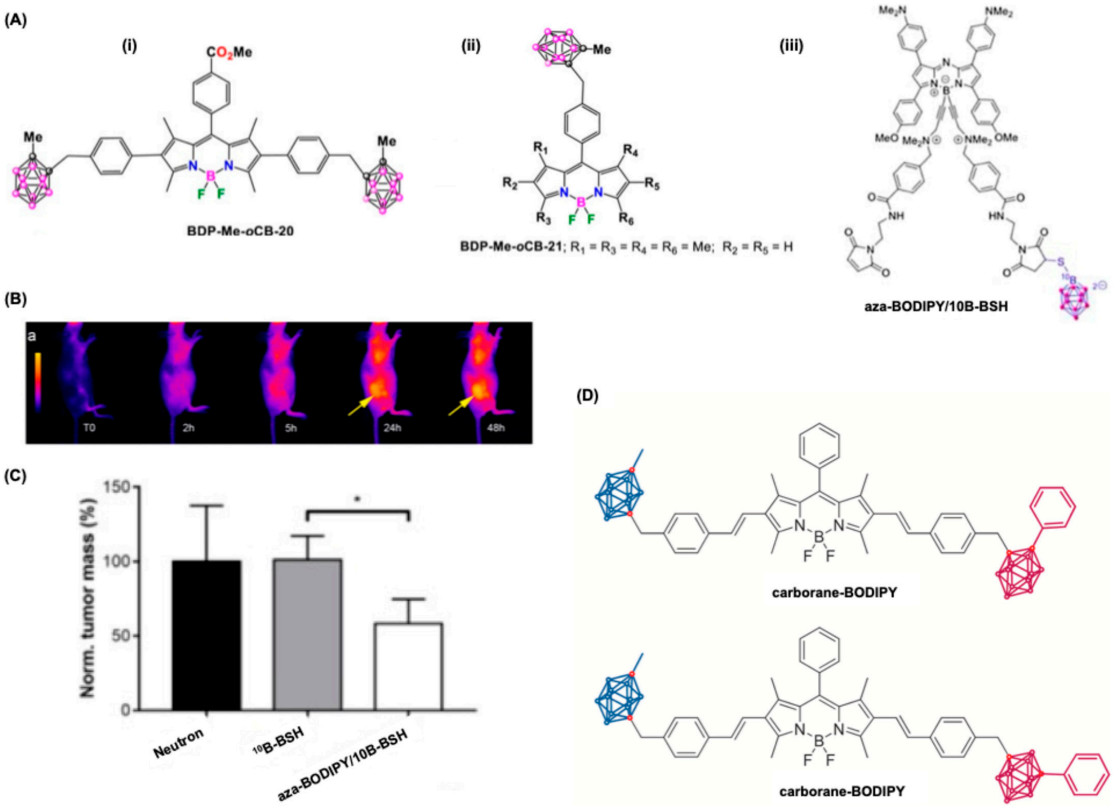


Figure 16. Various carborane-BODIPY derivatives for Boron Neutron Capture Therapy. (**A**) Represents the chemical structure for (**i**) BDP-Me-oCB-20 and (**ii**) BDP-Me-oCB-21, respectively. (**iii**) Chemical structure for aza-BODIPY/10B-BSH. (**B**) In vivo distribution and behavior of aza-BODIPY-10B-BSH in mice-bearing subcutaneous U-87 MG tumors at various time points. Arrows indicate the tumor region in the mice. (**C**) Represents the tumor growth after 16 days of post treatment using aza-BODIPY-10B-BSH, and various controls with an exposure of neutrons for 1 h. Statistical significance: * $p < 0.05$ (**D**) Chemical structure for the carborane-BODIPY derivatives for BNCT. Reproduced with permission from [110], 2015, Elsevier; [111], 2020, MDPI; [112], 2021, Elsevier, respectively.

One of the primary advantages of using BODIPY derivatives in BNCT is their versatile photophysical properties, which can be tailored through chemical modifications. These optoelectronic characteristics allow BODIPYs to be engineered for enhanced solubility, stability, and tumor-targeting capabilities. For example, aza-BODIPY, a BODIPY variant, has been developed that emits in the near-infrared (NIR) region, which is advantageous for in vivo optical imaging due to its deeper tissue penetration and lower autofluorescence of biological tissues. Additionally, aza-BODIPY can form stable conjugates with boron-containing compounds such as sodium borocaptate (10B-BSH), improving the delivery of boron into tumors and facilitating real-time imaging of its biodistribution within the body (Figure 16A(iii)) [111]. The newly developed aza-BODIPY/10B-BSH compound, for instance, has been demonstrated to achieve high tumor accumulation due to its favorable physicochemical properties, while simultaneously conveying imaging capabilities for monitoring its delivery and distribution. Clinical trials exploring the potential of BODIPY-based BNCT have yielded promising results, particularly for the treatment of solid tumors such as glioblastoma and head and neck cancers (Figure 16B,C). In preclinical models, the use of aza-BODIPY/10B-BSH conjugates has shown improved therapeutic efficacy as compared to conventional boron carriers like 10B-BSH alone. Studies reveal that tumor growth was significantly reduced when treated with the aza-BODIPY-conjugated boron agents combined with neutron irradiation (Figure 16C). This advancement not only underscores the effectiveness of BODIPY in enhancing BNCT but also positions it as a potential frontrunner in the search for targeted therapies against challenging cancers that are resistant to conventional treatments [111]. Bellomo et al. fabricated a library of 2,6- and 3,5-distyrenyl-substituted carborane-BODIPY dyes with excellent NIR absorption and photostability (Figure 16D) [112]. The attachment of BODIPY unit to carborane enhanced the boron content for BNCT as suggested.

6. BODIPY Based Nanomedicines for Theragnostic Applications

Owing to good photostability, fluorescence and therapeutical applications, the use of BODIPY for biological applications is still challenging due to the hydrophobicity of most of the dyes, or special synthetic routes needed for making them water soluble. Advancements in nanotechnology overcome these issues and various BODIPY-based nanoparticles (BDP-NPs) have been prepared recently for biomedical applications [33,113,114]. Controlling the aggregation property of BODIPY (J or H-aggregates) using the nanoprecipitation method allows the fabrication of a library of BDPNPs for bioimaging and therapeutical applications [115–118]. The aggregation enhances the emission and photosensitization properties of such dyes for biomedical applications. Another strategy is that BODIPY dyes can directly conjugate with metallic NPs for various biomedical applications [119–124].

6.1. Self-Assembled BDPNPs for Bioimaging and Therapeutical Applications

To prepare self-assembled BDPNPs, the nanoprecipitation technique is mostly used, in which a miscible solution of dye in acetone, methanol, tetrahydrofuran, etc., is added dropwise to water under stirring conditions and the organic solvent is evaporated slowly, followed by dialysis and centrifuge; the precipitated NPs are collected and redispersed in water for various applications. As shown in Figure 17A, the self-assembled NPs can be used for various biomedical applications.

In recent developments within the field of photodynamic therapy and bioimaging, BDPNPs have emerged as significant agents due to their impressive optical properties and biocompatibility. A series of BDPNPs were prepared from various BODIPY dyes as shown in Figure 17B.

A stable nanoparticle composed of a BODIPY dimer, specifically BDP 1, was reported by Z. Li et al. [125]. These nanoparticles were synthesized using a structure that combined the BODIPY dye with tetraphenylethene, resulting in nanoparticles with an approximate diameter of 110 nm, as measured by both transmission electron microscopy and scanning electron microscopy. Importantly, the photostability of BDP 1 nanoparticles showed noteworthy enhancements compared to their monomeric counterparts when assessed under UV light irradiation in tetrahydrofuran. This photostability is a crucial factor for their practical application in cellular environments. The cellular imaging capabilities of BDP 1 nanoparticles were evaluated using confocal laser scanning microscopy on human cervical carcinoma (HeLa) cells, revealing bright red fluorescence localized in the cytoplasm. This highlighted the potential of BDP 1 nanoparticles for effective imaging in biological systems, paving the way for further research and applications. Building upon these findings, Liu et al. synthesized two additional BODIPY derivatives, BDP 2 and BDP 3, which also demonstrated the ability to self-assemble into nanoparticles, achieving diameters of 112 nm and 98 nm, respectively (Figure 17C) [126]. A notable observation regarding BDP 2 NPs was their sensitivity to temperature, as their diameter expanded significantly from 112 nm to 2000 nm upon storage at room temperature for one month, indicating a potential instability issue. In contrast, BDP 3 NPs exhibited enhanced stability in aqueous environments. Of particular interest is the dual-emission characteristic of BDP 3 NPs, which displayed peaks at 566 nm and 683 nm upon excitation at 500 nm, contrasting with a maximum emission wavelength of 543 nm in THF. When THF was introduced to BDP 3 NPs in water, fluorescence spectroscopic analysis indicated an increase in intensity at 566 nm alongside a decrease at 683 nm, suggesting a transition from nanoparticle aggregates to individual molecules. According to dynamic light measurements, BDP3 NPs were eliminated from the medium with the addition of just 30% THF, underscoring their transformation dynamics in varying solvent conditions. Remarkably, BDP 3 NPs retained their proficiency for cellular imaging, with fluorescence localization confirmed within lysosomal compartments, thus indicating their effectiveness as imaging agents in live-cell applications (Figure 17D).

Xie's group explored whether BDP dimers with linkers could self-assemble into nanoparticles, offering stimuli-responsiveness and multifunctionality. They synthesized various BDP dimers, including BDP 4 with a disulfide bond via the Passerini reaction [127]. BDP 4 formed stable nanocapsules (~200 nm) in aqueous solutions, exhibiting reduction and light sensitivity. BDP 5, containing diselenide, formed nanoparticles (~160 nm) with strong reduction-responsiveness and bioimaging capability [128]. It expanded in size with glutathione (GSH) and showed enhanced fluorescence in cells. Additionally, BDP 5 coassembled with paclitaxel dimer, showed selectively towards tumor cells. BDP 6, with longer alkyl linkers, maintained colloidal stability in biological conditions, unlike shorter-linker dimers [129].

Kumar et al. fabricated a hexaiodo BODIPY with efficient photostability and self-assembling properties (Figure 17E) [118]. The incorporation of iodine atoms quenched the fluorescence of BODIPY dye in solution, but the self-assembled nano aggregates (BDP 7) enhanced the emission and photosensitization property of this BODIPY dye. The nano aggregates showed a singlet oxygen quantum yield of 0.82, which is higher than commercially available methylene blue. Owing to the high singlet oxygen quantum yield, the nanoaggregates used for PDT studies and results showed ~60% cell death for C6 cells after irradiation of NPs with laser (Figure 17F). Owing to the enhanced emission property, the nanoaggregates were used for cell imaging using different laser excitations such as 405/488/561 nm simultaneously (Figure 17G).

These findings collectively depict the advancement in BODIPY nanoparticle technology, demonstrating their significance as versatile tools in both imaging and therapeutic modalities in cancer treatment.

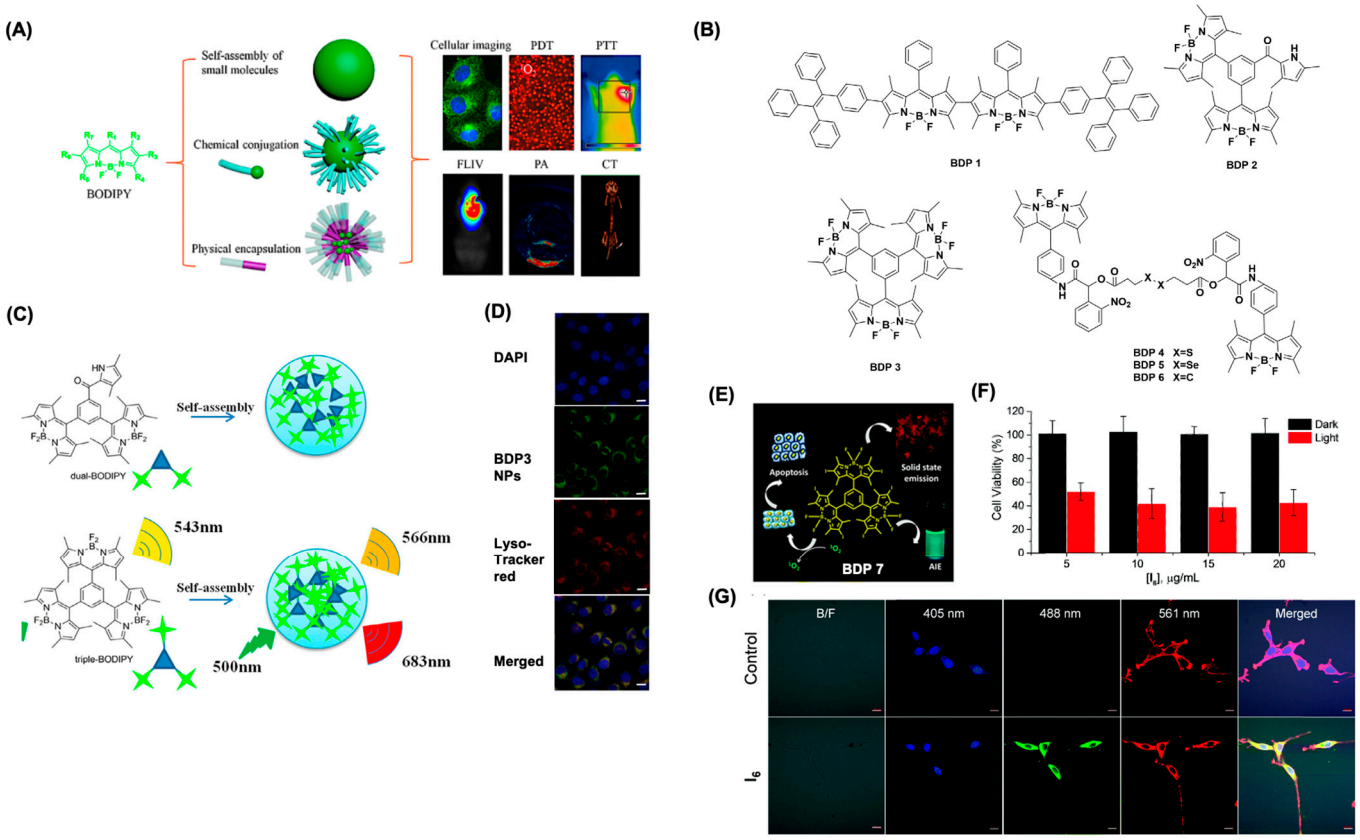


Figure 17. Self-assembled BODIPY dyes for biomedical applications. (**A**) A general scheme for the application of BDPNPs for various cellular imaging and therapeutical applications. (**B**) Chemical structure for various BODIPY dyes used for nanoparticle formations. (**C**) A schematic for the self-assembling process in BODIPY dye for the formation of BDP-2 and BDP-3 NPs. (**D**) Confocal laser microscopy images of HeLa cells costained with BDP-3-NPs (5 μM) and Lyso-Tracker Red. The images show the fluorescence of nuclei (blue), TBDP-NPs (green), Lyso-Tracker Red (red) and merged images (yellow) from left to right. Scale bar 100 μM. (**E**) A cartoon representation of the structure of hexa-Iodo BODIPY dye and its applications for PDT and cellular imaging. (**F**) In vitro phototoxicity in C6 cells treated with Hexaiodo BODIPY nanoaggregate under dark and light conditions. (**G**) Confocal microscopic image of C6 cells treated with Hexaiodo BODIPY nanoaggregate (12.5 μg mL^{-1}) excited at different wavelengths (green and red color). The cells were stained with nuclear staining dye Hoechst 33,342 (blue color) and phalloidin-TRITC. Scale bar is 10 μm. Reproduced with permission from [114], 2020, Wiley; [126], 2017, Elsevier; [118], 2020, RSC Publishing group, respectively.

6.2. Physical Encapsulation of BODIPY to Form BDNPs

Due to the hydrophobicity and extended pi conjugated backbones BODIPY dyes can be easily entrapped into various liposomes, polymers, etc., for the fabrication of BDP NPs (Figure 18). In one of the studies, carbazole-BODIPY dye (BDP 8) was entrapped into PLGA-Folic acid conjugate for the fabrication of BDPNPs. The NPs showed an average size of 20 nm with excellent stability for days with enhanced NIR emission [130]. PDT studies on the subcutaneous 4T1 tumor xenograft model showed that this NPS can suppress the growth of 8 mm sized tumors with efficient singlet oxygen generations and showed enhanced bioimaging capability. In another study, Huang, Li, et al., showed that conjugating two BODIPY units using a triazole link can act as a FRET pair (BDP 9) with 1.9-fold enhanced in singlet oxygen generation rather than the monoderivative. Amphiphilic pluronic surfac-

tant with folic acid conjugate was used as a matrix to improve the solubility of the dye, and in vitro and in vivo studies showed the NPs can kill HeLa cells rather than normal cells [131]. Naim et al. reported a supramolecular nanocomposite from BODIPY, tetra iodoethylene, embedded into a chitosan matrix for enchanted singlet oxygen generation (BDP 10) [132]. Nanocomposite showed excellent photostability, as compared to individual components, and reduced cytotoxicity for bio applications. The use of tetra iodoethylene is crucial since it enhances the intersystem crossing of the nanomaterial for photosensitization. The water-soluble nanomaterial showed an average particle size of between 250 and 330 nm, with a singlet oxygen quantum yield of 0.12. In vitro tumor studies (C6 cells) showed 39% cell viability after irradiating the nanomaterial with white light (80 mW cm^{-2}) for 30 min.

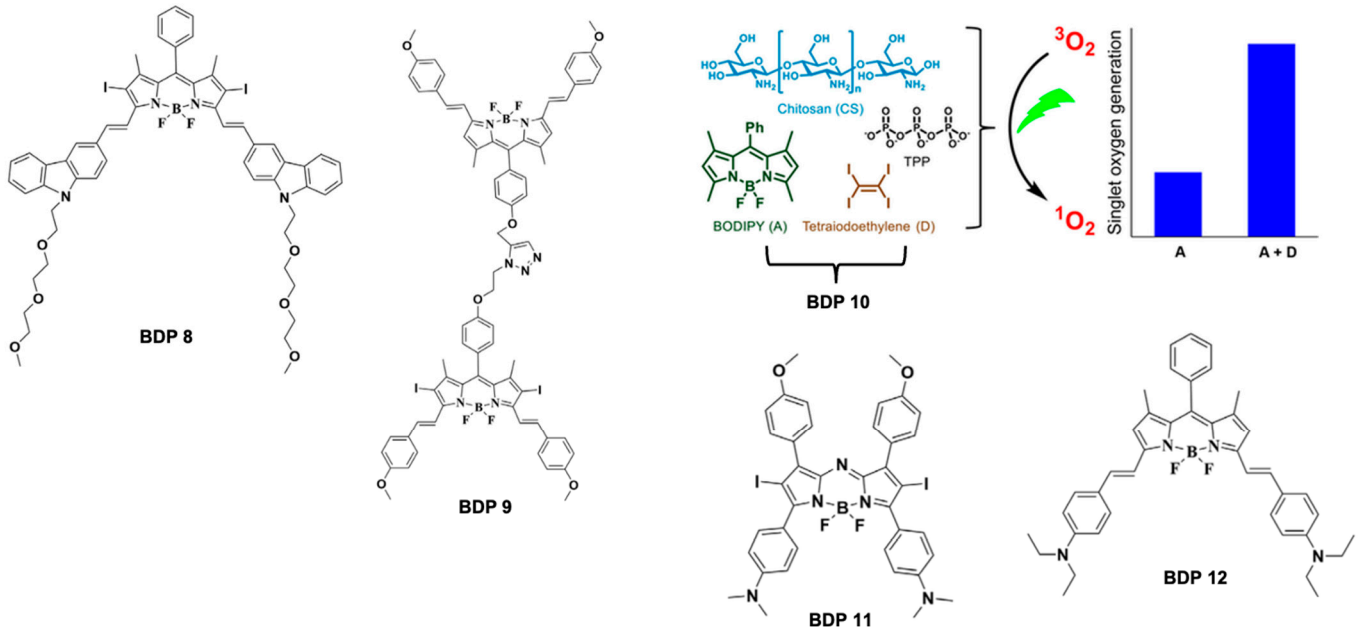


Figure 18. Chemical structures for various BODIPY derivatives for the formation of BDPNPS using polymer matrixes.

BODIPY compounds have garnered significant attention due to their responsiveness to the tumor microenvironment, particularly those that are pH sensitive. Among these, the aza-BODIPY reported by Dong's group features a dimethylaminophenyl group, enhancing its utility in biomedical applications (BDP 11) [133]. The NPs formed from this compound, BDP 11, exhibit a diameter of approximately 30 nm and are created using a combination of hydrophobic BDP 11 and amphiphilic DSPE-mPEG2000, an agent that facilitates better solubility and stability in physiological conditions. As the pH of the surrounding environment decreases from 7.4 to 5.0, BDP 11 NPs display enhanced capabilities in photoacoustic imaging, as well as photodynamic and photothermal effects. These improvements were confirmed through both in vitro and in vivo studies, demonstrating the potential of these NPs for effective tumor visualization and treatment. Furthermore, research by Lin et al. has expanded the applications of BODIPY compounds by integrating them with PEG–PLA for NIR fluorescence imaging, which boasts a high signal-to-noise ratio, along with PA and computed tomography functionalities [134]. This series of pH-sensitive BODIPY nanoparticles offers great promise for simultaneous imaging and therapeutic interventions.

Dong's team has also explored variations in the number of diethylaminophenyl groups attached to BODIPY, which further heighten its pH sensitivity compared to compounds with dimethylaminophenyl groups [135]. Notably, the introduction of two diethylaminophenyl groups in BDP 12 resulted in a marked red shift of the absorption and fluorescence emis-

sion wavelengths, enhancing tissue penetration. Following a similar preparation with DSPE-mPEG2000, BDP 12 NPs achieved an absorption peak in the NIR range at 735 nm. Additionally, under illumination with a 730 nm laser, BDP 11 NPs demonstrated an increase in temperature from 19.5 to 22.3 °C, accompanied by a pH drop from 7.4 to 5.5, indicative of an enhanced photothermal response. This pH/ROS-activated strategy highlights the dual utility of these BODIPY NPs, making them promising candidates for fluorescence-guided PDT and PTT in cancer management. Through these advancements, pH-sensitive BODIPY nanoparticles not only facilitate improved imaging and therapeutic efficacy but also pave the way for more targeted and effective cancer therapies.

6.3. Supramolecular Approach Using Metallic Nanoparticles

The integration of metallic nanoparticles with BODIPY dyes has opened promising avenues in the fields of cancer imaging and therapy. Suitable designs from BODIPY dyes which can anchor with metallic NPs can exhibit enhanced properties, including improved localization in tumor tissues and increased efficiency in light-activated therapeutic mechanisms [33].

Metallic nanoparticles, such as gold and silver, offer unique optical properties due to their surface plasmon resonance, which can be exploited to enhance the photodynamic effects of BODIPY dyes. These nanoparticles can accumulate preferentially in tumor tissues due to the EPR effect, thereby facilitating targeted delivery of the BODIPY dyes directly to malignant cells [136]. Studies have shown that gold nanoparticles fused with BODIPY derivatives can act both as imaging agents and therapeutic agents, providing dual functionality [98,137]. For instance, BODIPY-conjugated gold nanoparticles have been effectively used as fluorescent sensors in in vitro models of cancer, enabling real-time imaging of biological processes specific to tumor development [138]. Uniform polyethyleneimine-coated magnetic Fe_3O_4 nanoparticles were synthesized via a modified co-precipitation method and covalently conjugated with the BODIPY fluorophore using DCC/DMAP coupling reactions. The NPs showed imaging capability and were tested for the first time on human cancer cells (A549 and Ishikawa), while cytotoxicity was assessed on both cancer and healthy HUVEC cells using the MTT assay. Additionally, the nanoparticles' in vitro activities were evaluated and suggested they can be used for future MRI applications.

Kim and colleagues designed an innovative drug delivery platform utilizing gold monolayer nanoparticles [139]. Their approach incorporated "hydrophobic pockets", previously identified by Lucarini and Pasquato, to facilitate effective payload encapsulation. Zwitterionic chains were grafted onto the gold surface, creating spaces to load BODIPY molecules as fluorescent markers. The study revealed that the dye transfer occurs via a monolayer-membrane interaction mechanism. Additionally, the nanoparticles exhibited minimal uptake in MCF-7 human breast cancer cells. However, significant cytosolic delivery was observed within two hours of incubation. Notably, the BODIPY-loaded nanoparticles demonstrated remarkable stability, retaining their integrity for over a month.

In PDT studies, incorporation of AuNPs with BODIPY dye showed enhanced therapeutical and bioimaging applications. For instance, Kumar et al. showed a series of design strategies in which AuNPs can be incorporated with BODIPY dyes and controlling their structure–activity relationships the photophysics and fluorescence of these nanomaterials can be controlled for various applications [120]. Use of tryptophan-reduced AuNPs as a matrix, the simple BODIPY dye can be incorporated into the AuNPs via various supramolecular interactions (Figure 19A). The nanomaterial showed enhanced photostability and quenched fluorescence from BODIPY with a singlet oxygen quantum yield of $\Phi\Delta = 0.46$. These nanomaterials showed an enhanced PDT effect towards C6 cells with a phototoxicity of 85% without cytotoxic to normal cells (Figure 19B,C) [123]. This work has been extended using the interplay between BODIPY structures and a FRET-based nanocom-

posite is prepared (NC3). NC1 is prepared using BODIPY 1 and AuNPs, while NC2 is prepared using a Iodo pentamethyl BODIPY dye (2) and AuNPs. NC3 is prepared using two different BODIPY dyes such as pentamethyl BODIPY dye (1) and Iodo pentamethyl BODIPY dye (2) with AuNPs. Under the light, NC3 nanocomposites showed enhanced luminescence on the surface of AuNPs via a distinct radio decay pathway, and this property was used for simultaneous cell imaging and PDT studies (Figure 19D). The nanocomposite showed a singlet oxygen quantum yield of $\Phi\Delta = 0.68$, which is comparable with known dye methylene blue, but the nanocomposite showed excellent photostability comparable with the known dye methylene blue [120]. Detection of biothiols in tumor cells is important since an elevated biothiol concentration is present in tumor cells. Using an indicator displacement approach, in which the BODIPY dyes were non-fluorescent on the surface of AuNPs, displaces the BODIPY from the metallic surface after interaction with biothiols, and shows a fluorescent turn-on for BODIPY dyes (Figure 19E). Such a design strategy is used for cancer cell imaging and quantification of biothiols in tumor cells [122,124].

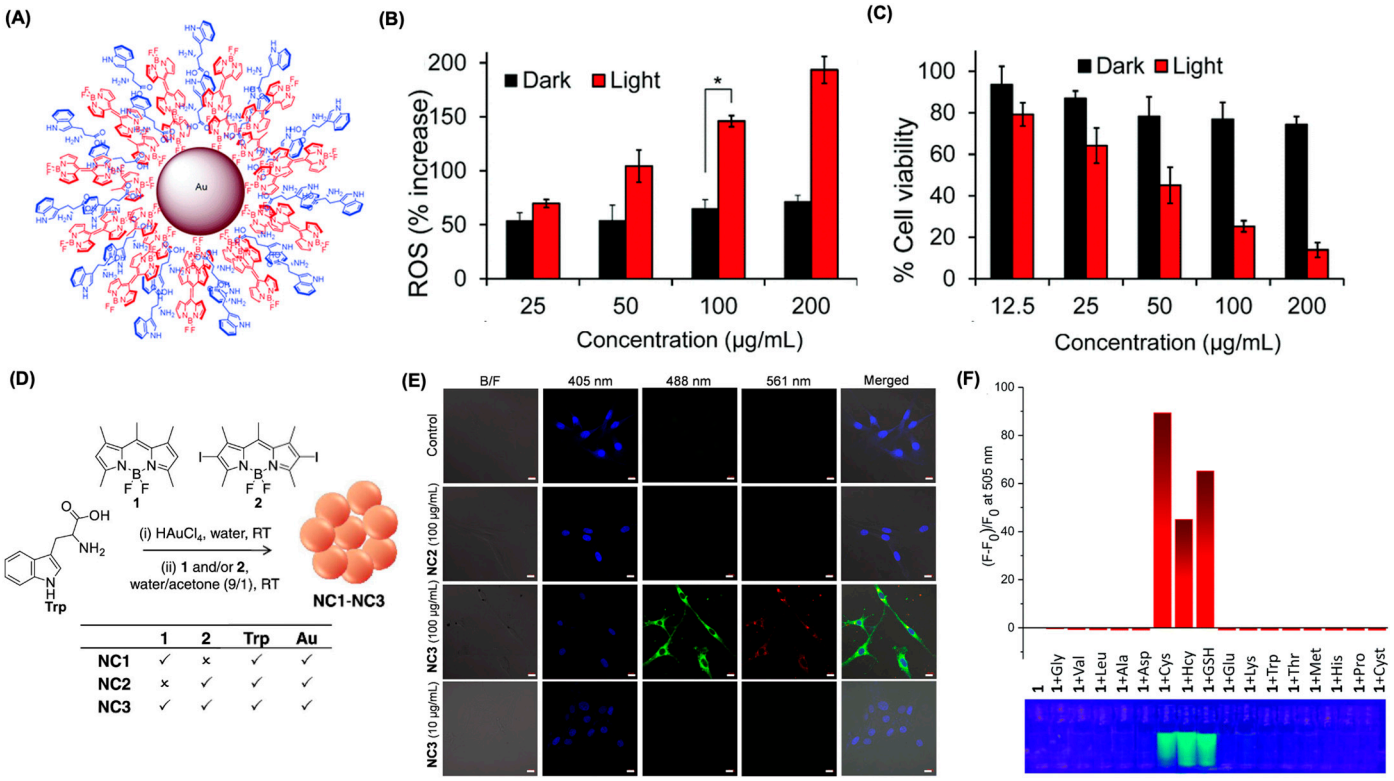


Figure 19. Fabrication of BODIPY nanoparticles using gold nanoparticles as a matrix. (**A**) A pictorial representation for the formation of nanocomposite from Pyrrole BODIPY and tryptophan. (**B**) Quantification of intracellular ROS in C6 cells treated with Pyrrole BODIPY-Au NPs, and (**C**) Cytotoxicity of Pyrrole BODIPY-Au NPs against C6 cells under dark and light irradiation using a 36 W white LED. * Two-tailed *p* value equals 0.0001. (**D**) Schematic representation of a hybrid nanocomposite from two different BODIPY and AuNPs. The table indicates the composition of various nanocomposites prepared, such as NC1, NC2 and NC3. Simultaneous FRET and electron transfer from BODIPY aggregates 1 and 2 to gold resulting in fluorescence and singlet oxygen generation. (**E**) Confocal laser scanning microscopy images of nanocomposite NC2 and NC3 treated C6 glioma cells. B/F are bright-field images; 405, 488, and 561 nm are the wavelengths of the laser used to excite the nanocomposites. The scale bar is 10 μm. (**F**) represents the fluorescence "turn-on" from BODIPY dye after the biothiol interaction with the nanocomposite having BODIPY and AuNPs. The nanoparticles were non-fluorescent initially which showed "turn-on" fluorescence after interaction of biothiols with gold, and the BODIPY dye displaced from the surface of Au regains its fluorescence. Reproduced with permission from [123], 2019, RSC publishing group; [120], 2022, ACS, respectively.

Overall, the combination of metallic nanoparticles and BODIPY dyes represents a powerful strategy for advancing cancer imaging and therapy, leveraging their complementary strengths to improve diagnostic capabilities and therapeutic efficacy in oncological applications. This innovative approach not only facilitates early detection and precise monitoring of cancers but also enhances therapeutic responses, thereby paving the way for more effective cancer treatment modalities.

7. Summary and Conclusions

The utilization of BODIPY dyes and their nanoparticles in cancer imaging and therapeutics represents a promising frontier in modern oncology, driven by the inherent optical properties and versatility of these compounds. BODIPY derivatives have been recognized for their strong absorption and emission characteristics in both the visible and near-infrared regions, making them highly effective fluorescent probes for imaging applications. Their excellent photostability and high quantum yield are pivotal for enhancing imaging fidelity, thus facilitating accurate diagnosis and treatment monitoring. Furthermore, BODIPY dyes can be engineered to target specific cancer cells, minimizing damage to surrounding healthy tissues, which is a crucial advancement over traditional therapies that often lack precision.

In recent developments, BODIPY nanoparticles have emerged as a powerful platform for photodynamic therapy (PDT), providing a synergistic approach to cancer treatment. By generating reactive oxygen species (ROS) upon light activation, these nanoparticles can effectively induce cell death in cancerous tissues while maintaining a favorable safety profile. Their ability to enhance cellular uptake and selectively accumulate in tumor microenvironments, aided by the Enhanced Permeability and Retention effect, significantly augments their therapeutic efficacy. Despite their potential, challenges remain, including the need for improved water solubility and selectivity of BODIPY photosensitizers. Ongoing research focuses on addressing these limitations through innovative modifications and the development of multifunctional nanoparticles that can cater to both diagnostic and therapeutic needs simultaneously.

In conclusion, BODIPY dyes and their nanoparticles hold great promise in revolutionizing cancer imaging and therapies, offering novel approaches that may enhance patient outcomes by improving diagnosis accuracy and treatment precision. As research continues to uncover the full potential of these compounds, they are likely to play an increasingly significant role in the future of cancer care, paving the way for more effective, targeted, and less invasive treatment modalities.

8. Future Outlook for BODIPY Dyes and Nanoparticles in Cancer Imaging and Therapy

The field of cancer treatment has seen significant advancements, but challenges remain in accurately detecting and effectively treating various types of cancer. BODIPY dyes, known for their superior photophysical properties, and BODIPY nanoparticles present great promise in enhancing cancer imaging and therapeutic applications. This essay discusses the outlook and potential developments regarding the use of BODIPY dyes and nanoparticles in tackling cancer challenges.

8.1. Enhanced Targeting and Delivery Mechanisms

One of the primary areas of advancement for BODIPY-based nanoparticles lies in enhancing targeting mechanisms and drug delivery systems. The unique properties of BODIPY dyes, such as their strong absorption in the visible and near-infrared regions, can be effectively exploited using nanoparticles that can preferentially accumulate in tumor tissues. Future research should focus on engineering nanoparticles that are responsive to specific

biological stimuli within the tumor environment, including pH, enzymatic activity, or hypoxic conditions. This will enhance the targeted delivery of BODIPY-based therapeutics, minimizing adverse effects on healthy tissues while improving therapeutic efficacy [6,140].

8.2. Integration of Theranostic Applications

The integration of therapeutic and diagnostic functionalities into a single platform, termed theragnostic, represents a promising direction for BODIPY dyes and nanoparticles. The development of BODIPY conjugates that exhibit both imaging capabilities and therapeutic action can significantly speed up the clinical translation of cancer therapies. The ability to perform real-time monitoring of drug effectiveness using fluorescence imaging while administering treatment could allow for more personalized and timely interventions. Recent advancements in BODIPY-based theragnostic systems are encouraging, with preliminary studies showing their potential to provide dual functionality in cancer imaging and therapy [31].

8.3. Innovations in Photodynamic Therapy (PDT)

BODIPY dyes have emerged as highly efficient photosensitizers for photodynamic therapy (PDT). Future advancements will likely focus on improving the efficacy of BODIPY-based PDT by optimizing their chemical structures to enhance singlet oxygen generation, thereby increasing their phototoxicity towards cancer cells [81]. Furthermore, combining BODIPY dyes with other therapeutic modalities, such as chemotherapy or immunotherapy, could lead to synergistic effects, providing a multifaceted approach to cancer treatment [141]. For instance, incorporating BODIPY dyes into existing chemotherapy protocols has demonstrated improved selectivity and reduced side effects due to their targeting capabilities [142]. Progressing nanotechnology will improve targeted cancer treatment, overcoming hurdles in its clinical implementation.

8.4. Development of Novel BODIPY Derivatives

Ongoing research into modifying the core structure of BODIPY molecules has the potential to revolutionize their applications in cancer therapy. Structural modifications can yield new derivatives with carefully tailored properties, such as altered solubility profiles, emission wavelengths, and enhanced stability under biological conditions. Innovations in synthetic techniques, such as click chemistry, can facilitate the creation of libraries of BODIPY derivatives, leading to the identification of optimal candidates for specific applications.

8.5. Utilization of BODIPY in Combination with Nanotechnology

The intersection of BODIPY chemistry and nanotechnology opens new avenues for cancer imaging and treatment. Nanotechnology not only enables enhanced stability and solubility of BODIPY dyes but also aids in the creation of multifunctional nanocarriers capable of delivering multiple therapeutic agents. Additionally, the development of targeted nanosystems that can respond to specific tumor markers offers a promising pathway for the precise delivery of BODIPY dyes, enhancing their role in both imaging and therapy.

8.6. Addressing Challenges

BODIPY dyes showcase exceptional capabilities in bioimaging and therapeutic applications; however, several significant disadvantages remain that hinder their clinical implementation. Limitations in absorption properties, coupled with hydrophobicity and potential for photobleaching raise critical concerns about their efficacy and reliability in medical settings. Additionally, cytotoxicity concerns and the complexities of structural optimization further constrain their application in clinical trials. Future research must focus on overcoming these challenges to facilitate the translation of BODIPY-based technologies

from the laboratory to the clinic. The establishment of clear regulatory pathways and guidelines for the use of nanoparticles in medical applications will be critical in this regard [143]. The ongoing development of advanced targeting mechanisms, innovative theragnostic platforms, and novel chemical derivatives will likely enhance their efficacy and applicability. By addressing current challenges and optimizing their properties, BODIPY-based technologies could play a transformative role in the fight against cancer, leading to improved diagnostic capabilities and more effective therapies for patients worldwide. As research continues to advance, BODIPY dyes are poised to become integral components of the next generation of cancer treatments.

Author Contributions: Conceptualization P.P.P.K.; resources, P.P.P.K.; data curation, S.S., R.J. and P.P.P.K.; writing—original draft preparation P.P.P.K.; writing—review and editing, S.S., R.J. and P.P.P.K.; supervision, P.P.P.K. All authors have read and agreed to the published version of the manuscript.

Funding: This research received no external funding.

Acknowledgments: P.P.P.K. shows sincere gratitude to the Department of Biomedical Engineering, Michigan State University, for the facilities and use of resources for the literature collections.

Conflicts of Interest: Author Rakesh Joshi was employed by the company DARVUN. The remaining authors declare that the research was conducted in the absence of any commercial or financial relationships that could be construed as a potential conflict of interest.

References

1. Kowada, T.; Maeda, H.; Kikuchi, K. BODIPY-Based Probes for the Fluorescence Imaging of Biomolecules in Living Cells. *Chem. Soc. Rev.* **2015**, *44*, 4953–4972. [CrossRef]
2. Samanta, S.; Lai, K.; Wu, F.; Liu, Y.; Cai, S.; Yang, X.; Qu, J.; Yang, Z. Xanthene, Cyanine, Oxazine and BODIPY: The Four Pillars of the Fluorophore Empire for Super-Resolution Bioimaging. *Chem. Soc. Rev.* **2023**, *52*, 7197–7261. [CrossRef] [PubMed]
3. Lu, H.; Mack, J.; Yang, Y.; Shen, Z. Structural Modification Strategies for the Rational Design of Red/NIR Region BODIPYs. *Chem. Soc. Rev.* **2014**, *43*, 4778–4823. [CrossRef] [PubMed]
4. Treibs, A.; Kreuzer, F. Difluorboryl-Komplexe von Di- Und Tripyrrylmethenen. *Justus Liebigs Ann. Chem.* **1968**, *718*, 208–223. [CrossRef]
5. Krasnopyorov, A.I.; Larkina, E.A. Features of F2-BODIPY Synthesis (A Review). *Russ. J. Org. Chem.* **2024**, *60*, 789–805. [CrossRef]
6. Das, S.; Dey, S.; Patra, S.; Bera, A.; Ghosh, T.; Prasad, B.; Sayala, K.D.; Maji, K.; Bedi, A.; Debnath, S. BODIPY-Based Molecules for Biomedical Applications. *Biomolecules* **2023**, *13*, 1723. [CrossRef]
7. Kaur, P.; Singh, K. Recent Advances in the Application of BODIPY in Bioimaging and Chemosensing. *J. Mater. Chem. C* **2019**, *7*, 11361–11405. [CrossRef]
8. Ahmad, H.; Muhammad, S.; Mazhar, M.; Farhan, A.; Iqbal, M.S.; Hiria, H.; Yu, C.; Zhang, Y.; Guo, B. Unveiling Cellular Mysteries: Advances in BODIPY Dyes for Subcellular Imaging. *Coord. Chem. Rev.* **2025**, *526*, 216383. [CrossRef]
9. Yadav, I.S.; Misra, R. Design, Synthesis and Functionalization of BODIPY Dyes: Applications in Dye-Sensitized Solar Cells (DSSCs) and Photodynamic Therapy (PDT). *J. Mater. Chem. C* **2023**, *11*, 8688–8723. [CrossRef]
10. Loudet, A.; Burgess, K. BODIPY Dyes and Their Derivatives: Syntheses and Spectroscopic Properties. *Chem. Rev.* **2007**, *107*, 4891–4932. [CrossRef]
11. Schäfer, C.; Mony, J.; Olsson, T.; Börjesson, K. Effect of the Aza-N-Bridge and Push–Pull Moieties: A Comparative Study between BODIPYs and Aza-BODIPYs. *J. Org. Chem.* **2022**, *87*, 2569–2579. [CrossRef] [PubMed]
12. Shi, Z.; Han, X.; Hu, W.; Bai, H.; Peng, B.; Ji, L.; Fan, Q.; Li, L.; Huang, W. Bioapplications of Small Molecule Aza-BODIPY: From Rational Structural Design to in Vivo Investigations. *Chem. Soc. Rev.* **2020**, *49*, 7533–7567. [CrossRef]
13. Dutta, D.; Nair, R.R.; Mangalath, S.; Nair, S.A.; Joseph, J.; Gogoi, P.; Ramaiah, D. Biocompatible Aza-BODIPY-Biotin Conjugates for Photodynamic Therapy of Cancer. *ACS Omega* **2023**, *8*, 26180–26190. [CrossRef]
14. Elgun, T.; Yurttas, A.G.; Cinar, K.; Ozcelik, S.; Gul, A. Effect of Aza-BODIPY-Photodynamic Therapy on the Expression of Carcinoma-Associated Genes and Cell Death Mode. *Photodiagnosis Photodyn. Ther.* **2023**, *44*, 103849. [CrossRef]
15. Hlogyik, T.; Laczkó-Rigó, R.; Bakos, É.; Poór, M.; Kele, Z.; Özvegy-Laczka, C.; Mernyák, E. Synthesis and in Vitro Photodynamic Activity of Aza-BODIPY-Based Photosensitizers. *Org. Biomol. Chem.* **2023**, *21*, 6018–6027. [CrossRef] [PubMed]
16. Li, K.; Duan, X.; Jiang, Z.; Ding, D.; Chen, Y.; Zhang, G.-Q.; Liu, Z. J-Aggregates of Meso-[2.2]Paracyclophanyl-BODIPY Dye for NIR-II Imaging. *Nat. Commun.* **2021**, *12*, 2376. [CrossRef] [PubMed]

17. Hu, X.; Fang, Z.; Zhu, C.; Yang, Y.; Yang, Z.; Huang, W. Crucial Breakthrough of BODIPY-Based NIR-II Fluorescent Emitters for Advanced Biomedical Theranostics. *Adv. Funct. Mater.* **2024**, *34*, 2401325. [CrossRef]
18. Bai, L.; Sun, P.; Liu, Y.; Zhang, H.; Hu, W.; Zhang, W.; Liu, Z.; Fan, Q.; Li, L.; Huang, W. Novel Aza-BODIPY Based Small Molecular NIR-II Fluorophores for in Vivo Imaging. *Chem. Commun.* **2019**, *55*, 10920–10923. [CrossRef]
19. Liu, Q.; Tian, J.; Tian, Y.; Sun, Q.; Sun, D.; Wang, F.; Xu, H.; Ying, G.; Wang, J.; Yetisen, A.K.; et al. Near-Infrared-II Nanoparticles for Cancer Imaging of Immune Checkpoint Programmed Death-Ligand 1 and Photodynamic/Immune Therapy. *ACS Nano* **2021**, *15*, 515–525. [CrossRef]
20. Yang, N.; Song, S.; Liu, C.; Ren, J.; Wang, X.; Zhu, S.; Yu, C. An Aza-BODIPY-Based NIR-II Luminogen Enables Efficient Phototheranostics. *Biomater. Sci.* **2022**, *10*, 4815–4821. [CrossRef]
21. Tian, Y.; Zhou, H.; Cheng, Q.; Dang, H.; Qian, H.; Teng, C.; Xie, K.; Yan, L. Stable Twisted Conformation Aza-BODIPY NIR-II Fluorescent Nanoparticles with Ultra-Large Stokes Shift for Imaging-Guided Phototherapy. *J. Mater. Chem. B* **2022**, *10*, 707–716. [CrossRef] [PubMed]
22. Bian, S.; Zheng, X.; Liu, W.; Li, J.; Gao, Z.; Ren, H.; Zhang, W.; Lee, C.-S.; Wang, P. Pyrrolopyrrole Aza-BODIPY-Based NIR-II Fluorophores for in Vivo Dynamic Vascular Dysfunction Visualization of Vascular-Targeted Photodynamic Therapy. *Biomaterials* **2023**, *298*, 122130. [CrossRef] [PubMed]
23. Tang, D.; Yu, Y.; Zhang, J.; Dong, X.; Liu, C.; Xiao, H. Self-Sacrificially Degradable Pseudo-Semiconducting Polymer Nanoparticles That Integrate NIR-II Fluorescence Bioimaging, Photodynamic Immunotherapy, and Photo-Activated Chemotherapy. *Adv. Mater.* **2022**, *34*, 2203820. [CrossRef] [PubMed]
24. Wan, J.; Zhang, X.; Tang, D.; Liu, T.; Xiao, H. Biodegradable NIR-II Pseudo Conjugate Polymeric Nanoparticles Amplify Photodynamic Immunotherapy via Alleviation of Tumor Hypoxia and Tumor-Associated Macrophage Reprogramming. *Adv. Mater.* **2023**, *35*, 2209799. [CrossRef]
25. Bu, F.; Kang, X.; Tang, D.; Liu, F.; Chen, L.; Zhang, P.; Feng, W.; Yu, Y.; Li, G.; Xiao, H.; et al. Enhancing Near-Infrared II Photodynamic Therapy with Nitric Oxide for Eradicating Multidrug-Resistant Biofilms in Deep Tissues. *Bioact. Mater.* **2024**, *33*, 341–354. [CrossRef]
26. Tian, Y.; Yin, D.; Cheng, Q.; Dang, H.; Teng, C.; Yan, L. Supramolecular J-Aggregates of Aza-BODIPY by Steric and π–π Nteractions for NIR-II Phototheranostics. *J. Mater. Chem. B* **2022**, *10*, 1650–1662. [CrossRef]
27. Zhu, Y.; Wu, P.; Liu, S.; Yang, J.; Wu, F.; Cao, W.; Yang, Y.; Zheng, B.; Xiong, H. Electron-Withdrawing Substituents Allow Boosted NIR-II Fluorescence in J-Type Aggregates for Bioimaging and Information Encryption. *Angew. Chem. Int. Ed.* **2023**, *62*, e202313166. [CrossRef]
28. Dang, H.; Yin, D.; Tian, Y.; Cheng, Q.; Teng, C.; Xu, Y.; Yan, L. In Situ Formation of J-Aggregate in the Tumor Microenvironment Using Acidity Responsive Polypeptide Nanoparticle Encapsulating Galactose-Conjugated BODIPY Dye for NIR-II Phototheranostics. *J. Mater. Chem. B* **2022**, *10*, 5279–5290. [CrossRef]
29. Li, F.-Z.; Wu, Z.; Lin, C.; Wang, Q.; Kuang, G.-C. Photophysical Properties Regulation and Applications of BODIPY-Based Derivatives with Electron Donor-Acceptor System. *Results Chem.* **2022**, *4*, 100384. [CrossRef]
30. Bumagina, N.A.; Antina, E.V. Review of Advances in Development of Fluorescent BODIPY Probes (Chemosensors and Chemodosimeters) for Cation Recognition. *Coord. Chem. Rev.* **2024**, *505*, 215688. [CrossRef]
31. Mao, Z.; Kim, J.H.; Lee, J.; Xiong, H.; Zhang, F.; Kim, J.S. Engineering of BODIPY-Based Theranostics for Cancer Therapy. *Coord. Chem. Rev.* **2023**, *476*, 214908. [CrossRef]
32. Kim, G.; Luo, Y.; Shin, M.; Bouffard, J.; Bae, J.; Kim, Y. Making the Brightest Ones Dim: Maximizing the Photothermal Conversion Efficiency of BODIPY-Based Photothermal Agents. *Adv. Healthc. Mater.* **2024**, *13*, 2400885. [CrossRef] [PubMed]
33. Koczorowski, T.; Glowacka-Sobotta, A.; Sysak, S.; Mlynarczyk, D.T.; Lesyk, R.; Goslinski, T.; Sobotta, L. BODIPY-Based Nanomaterials—Sensing and Biomedical Applications. *Appl. Sci.* **2022**, *12*, 7815. [CrossRef]
34. Chen, D.; Zhang, T.; Dong, X.; Mou, X. BODIPY Based Nanomedicine for Cancer Imaging and Phototherapy. *Colloid. Interface Sci. Commun.* **2025**, *64*, 100816. [CrossRef]
35. Zhu, J.; Tan, N.K.; Kikuchi, K.; Kaur, A.; New, E.J. BODIPY-based Fluorescent Indicators for Lipid Droplets. *Anal. Sens.* **2024**, *4*, e202300049. [CrossRef]
36. Fan, W.; Li, X. Using BODIPY FL-Sphingolipid Analogs to Study Sphingolipid Metabolism in Mouse Embryonic Stem Cells. *Bio-Protocol* **2022**, *12*, e4555. [CrossRef]
37. Jurgutis, D.; Jarockyte, G.; Poderys, V.; Dodonova-Vaitkuniene, J.; Tumkevicius, S.; Vysniauskas, A.; Rotomskis, R.; Karabanovas, V. Exploring BODIPY-Based Sensor for Imaging of Intracellular Microviscosity in Human Breast Cancer Cells. *IJMS* **2022**, *23*, 5687. [CrossRef]
38. Nusshold, C.; Uellen, A.; Bernhart, E.; Hammer, A.; Damm, S.; Wintersperger, A.; Reicher, H.; Hermetter, A.; Malle, E.; Sattler, W. Endocytosis and Intracellular Processing of BODIPY-Sphingomyelin by Murine CATH.a Neurons. *Biochim. Et Biophys. Acta (BBA)—Mol. Cell Biol. Lipids* **2013**, *1831*, 1665–1678. [CrossRef]

39. Qiu, B.; Simon, M. BODIPY 493/503 Staining of Neutral Lipid Droplets for Microscopy and Quantification by Flow Cytometry. *Bio-Protocol* **2016**, *6*, e1912. [CrossRef]
40. Listenberger, L.L.; Brown, D.A. Fluorescent Detection of Lipid Droplets and Associated Proteins. *CP Cell Biol.* **2007**, *35*, 24.2.1–24.2.11. [CrossRef]
41. Debela, D.T.; Muzazu, S.G.; Heraro, K.D.; Ndalama, M.T.; Mesele, B.W.; Haile, D.C.; Kitui, S.K.; Manyazewal, T. New Approaches and Procedures for Cancer Treatment: Current Perspectives. *SAGE Open Med.* **2021**, *9*, 20503121211034366. [CrossRef]
42. Lin, Q.; Buccella, D. Highly Selective, Red Emitting BODIPY-Based Fluorescent Indicators for Intracellular Mg^{2+} Imaging. *J. Mater. Chem. B* **2018**, *6*, 7247–7256. [CrossRef] [PubMed]
43. Kand, D.; Liu, P.; Navarro, M.X.; Fischer, L.J.; Rousso-Noori, L.; Friedmann-Morvinski, D.; Winter, A.H.; Miller, E.W.; Weinstain, R. Water-Soluble BODIPY Photocages with Tunable Cellular Localization. *J. Am. Chem. Soc.* **2020**, *142*, 4970–4974. [CrossRef]
44. Spangenburg, E.E.; Pratt, S.J.P.; Wohlers, L.M.; Lovering, R.M. Use of BODIPY (493/503) to Visualize Intramuscular Lipid Dropletsin Skeletal Muscle. *BioMed Res. Int.* **2011**, *2011*, 598358. [CrossRef]
45. Miao, W.; Yu, C.; Hao, E.; Jiao, L. Functionalized BODIPYs as Fluorescent Molecular Rotors for Viscosity Detection. *Front. Chem.* **2019**, *7*, 825. [CrossRef]
46. Ordóñez-Hernández, J.; Ferrusca-Martínez, F.; Jiménez-Sánchez, A. BODIPY-Derived Fluorescent Probes for Targeting and Tracking Lipid Droplets Dynamics. *Tetrahedron* **2024**, *168*, 134354. [CrossRef]
47. Tatenaka, Y.; Kato, H.; Ishiyama, M.; Sasamoto, K.; Shiga, M.; Nishitoh, H.; Ueno, Y. Monitoring Lipid Droplet Dynamics in Living Cells by Using Fluorescent Probes. *Biochemistry* **2019**, *58*, 499–503. [CrossRef]
48. Chen, J.; Yue, F.; Kuang, S. Labeling and Analyzing Lipid Droplets in Mouse Muscle Stem Cells. *STAR Protoc.* **2022**, *3*, 101849. [CrossRef]
49. Walter, E.R.H.; Lee, L.C.-C.; Leung, P.K.-K.; Lo, K.K.-W.; Long, N.J. Mitochondria-Targeting Biocompatible Fluorescent BODIPY Probes. *Chem. Sci.* **2024**, *15*, 4846–4852. [CrossRef]
50. Polita, A.; Stancikaitė, M.; Žvirblis, R.; Maleckaitė, K.; Dodonova-Vaitkūnienė, J.; Tumkevičius, S.; Shivabalan, A.P.; Valinčius, G. Designing a Green-Emitting Viscosity-Sensitive 4,4-Difluoro-4-Bora-3a,4a-Diaza-*s*-Indacene (BODIPY) Probe for Plasma Membrane Viscosity Imaging. *RSC Adv.* **2023**, *13*, 19257–19264. [CrossRef]
51. Collot, M.; Boutant, E.; Lehmann, M.; Klymchenko, A.S. BODIPY with Tuned Amphiphilicity as a Fluorogenic Plasma Membrane Probe. *Bioconjugate Chem.* **2019**, *30*, 192–199. [CrossRef]
52. Li, A.; Wang, F.; Li, Y.; Peng, X.; Liu, Y.; Zhu, L.; He, P.; Yu, T.; Chen, D.; Duan, M.; et al. Fluorination of Aza-BODIPY for Cancer Cell Plasma Membrane-Targeted Imaging and Therapy. *ACS Appl. Mater. Interfaces* **2025**, *17*, acsami.4c17943. [CrossRef]
53. Xiong, T.; Chen, Y.; Peng, Q.; Li, M.; Lu, S.; Chen, X.; Fan, J.; Wang, L.; Peng, X. Pyrazolone-Protein Interaction Enables Long-Term Retention Staining and Facile Artificial Biorecognition on Cell Membranes. *J. Am. Chem. Soc.* **2024**, *146*, 24158–24166. [CrossRef] [PubMed]
54. Melo, R.C.N.; D'Avila, H.; Wan, H.-C.; Bozza, P.T.; Dvorak, A.M.; Weller, P.F. Lipid Bodies in Inflammatory Cells: Structure, Function, and Current Imaging Techniques. *J. Histochem. Cytochem.* **2011**, *59*, 540–556. [CrossRef] [PubMed]
55. Courtis, A.M.; Santos, S.A.; Guan, Y.; Hendricks, J.A.; Ghosh, B.; Szantai-Kis, D.M.; Reis, S.A.; Shah, J.V.; Mazitschek, R. Monoalkoxy BODIPYs—A Fluorophore Class for Bioimaging. *Bioconjugate Chem.* **2014**, *25*, 1043–1051. [CrossRef]
56. Ni, Y.; Zeng, L.; Kang, N.; Huang, K.; Wang, L.; Zeng, Z.; Chang, Y.; Wu, J. *Meso* -Ester and Carboxylic Acid Substituted BODIPYs with Far-Red and Near-Infrared Emission for Bioimaging Applications. *Chem. A Eur. J.* **2014**, *20*, 2301–2310. [CrossRef]
57. Jiang, X.-D.; Gao, R.; Yue, Y.; Sun, G.-T.; Zhao, W. A NIR BODIPY Dye Bearing 3,4,4a-Trihydroxanthene Moieties. *Org. Biomol. Chem.* **2012**, *10*, 6861. [CrossRef]
58. Yang, Z.; Kang, D.H.; Lee, H.; Shin, J.; Yan, W.; Rathore, B.; Kim, H.-R.; Kim, S.J.; Singh, H.; Liu, L.; et al. A Fluorescent Probe for Stimulated Emission Depletion Super-Resolution Imaging of Vicinal-Dithiol-Proteins on Mitochondrial Membrane. *Bioconjugate Chem.* **2018**, *29*, 1446–1453. [CrossRef]
59. Gayathri, T.; Karnewar, S.; Kotamraju, S.; Singh, S.P. High Affinity Neutral Bodipy Fluorophores for Mitochondrial Tracking. *ACS Med. Chem. Lett.* **2018**, *9*, 618–622. [CrossRef]
60. Kesavan, P.E.; Pandey, V.; Raza, M.K.; Mori, S.; Gupta, I. Water Soluble Thioglycosylated BODIPYs for Mitochondria Targeted Cytotoxicity. *Bioorganic Chem.* **2019**, *91*, 103139. [CrossRef]
61. Yang, J.; Zhang, R.; Zhao, Y.; Tian, J.; Wang, S.; Gros, C.P.; Xu, H. Red/NIR Neutral BODIPY-Based Fluorescent Probes for Lighting up Mitochondria. *Spectrochim. Acta Part A Mol. Biomol. Spectrosc.* **2021**, *248*, 119199. [CrossRef]
62. Chauhan, N.; Koli, M.; Ghosh, R.; Majumdar, A.G.; Ghosh, A.; Ghanty, T.K.; Mula, S.; Patro, B.S. A BODIPY-Naphtholimine-BF_2 Dyad for Precision Photodynamic Therapy, Targeting, and Dual Imaging of Endoplasmic Reticulum and Lipid Droplets in Cancer. *JACS Au* **2024**, *4*, 2838–2852. [CrossRef]
63. De Jong, F.; Pokorny, J.; Manshian, B.; Daelemans, B.; Vandaele, J.; Startek, J.B.; Soenen, S.; Van Der Auweraer, M.; Dehaen, W.; Rocha, S.; et al. Development and Characterization of BODIPY-Derived Tracers for Fluorescent Labeling of the Endoplasmic Reticulum. *Dye. Pigment.* **2020**, *176*, 108200. [CrossRef]

64. Hoenke, S.; Brandes, B.; Csuk, R. Non-Cytotoxic Aza-BODIPY Triterpene Conjugates to Target the Endoplasmic Reticulum. *Eur. J. Med. Chem. Rep.* **2023**, *7*, 100099. [CrossRef]
65. Kumar, P.P.P.; Kaushal, S.; Lim, D.-K. Recent Advances in Nano/Microfabricated Substrate Platforms and Artificial Intelligence for Practical Surface-Enhanced Raman Scattering-Based Bioanalysis. *TrAC Trends Anal. Chem.* **2023**, *168*, 117341. [CrossRef]
66. Lim, D.-K.; Kumar, P.P.P. Recent Advances in SERS-Based Bioanalytical Applications: Live Cell Imaging. *Nanophotonics* **2024**, *13*, 1521–1534. [CrossRef] [PubMed]
67. Faulds, K.; McKenzie, F.; Smith, W.E.; Graham, D. Quantitative Simultaneous Multianalyte Detection of DNA by Dual-Wavelength Surface-Enhanced Resonance Raman Scattering. *Angew. Chem. Int. Ed.* **2007**, *46*, 1829–1831. [CrossRef]
68. Adarsh, N.; Ramya, A.N.; Maiti, K.K.; Ramaiah, D. Unveiling NIR Aza-Boron-Dipyrromethene (BODIPY) Dyes as Raman Probes: Surface-Enhanced Raman Scattering (SERS)-Guided Selective Detection and Imaging of Human Cancer Cells. *Chem. A Eur. J.* **2017**, *23*, 14286–14291. [CrossRef]
69. Klapper, M.; Ehmke, M.; Palgunow, D.; Böhme, M.; Matthäus, C.; Bergner, G.; Dietzek, B.; Popp, J.; Döring, F. Fluorescence-Based Fixative and Vital Staining of Lipid Droplets in Caenorhabditis Elegans Reveal Fat Stores Using Microscopy and Flow Cytometry Approaches. *J. Lipid Res.* **2011**, *52*, 1281–1293. [CrossRef]
70. Xia, J.; Yao, J.; Wang, L.H.V. Photoacoustic tomography: Principles and advances (Invited Review). *Prog. Electromagn. Res.* **2014**, *147*, 1–22. [CrossRef]
71. Farooq, A.; Sabah, S.; Dhou, S.; Alsawaftah, N.; Husseini, G. Exogenous Contrast Agents in Photoacoustic Imaging: An In Vivo Review for Tumor Imaging. *Nanomaterials* **2022**, *12*, 393. [CrossRef]
72. Kumar, P.P.P.; Lim, D.-K. Photothermal Effect of Gold Nanoparticles as a Nanomedicine for Diagnosis and Therapeutics. *Pharmaceutics* **2023**, *15*, 2349. [CrossRef]
73. Ni, Y.; Kannadorai, R.K.; Peng, J.; Yu, S.W.-K.; Chang, Y.-T.; Wu, J. Naphthalene-Fused BODIPY near-Infrared Dye as a Stable Contrast Agent for in Vivo Photoacoustic Imaging. *Chem. Commun.* **2016**, *52*, 11504–11507. [CrossRef]
74. Ni, Y.; Kannadorai, R.K.; Yu, S.W.-K.; Chang, Y.-T.; Wu, J. Push–Pull Type Meso-Ester Substituted BODIPY near-Infrared Dyes as Contrast Agents for Photoacoustic Imaging. *Org. Biomol. Chem.* **2017**, *15*, 4531–4535. [CrossRef] [PubMed]
75. Miao, Q.; Lyu, Y.; Ding, D.; Pu, K. Semiconducting Oligomer Nanoparticles as an Activatable Photoacoustic Probe with Amplified Brightness for In Vivo Imaging of pH. *Adv. Mater.* **2016**, *28*, 3662–3668. [CrossRef]
76. Merkes, J.M.; Lammers, T.; Kancherla, R.; Rueping, M.; Kiessling, F.; Banala, S. Tuning Optical Properties of BODIPY Dyes by Pyrrole Conjugation for Photoacoustic Imaging. *Adv. Opt. Mater.* **2020**, *8*, 1902115. [CrossRef]
77. Ma, D.; Hou, S.; Bae, C.; Pham, T.C.; Lee, S.; Zhou, X. Aza-BODIPY Based Probe for Photoacoustic Imaging of ONOO− In Vivo. *Chin. Chem. Lett.* **2021**, *32*, 3886–3889. [CrossRef]
78. Ma, Y.; Cao, H.; Chen, B.; Xu, X.; Zhang, Q.; Chen, H.; Zhang, X.; Song, G. Simultaneous In Vivo Imaging of Neutrophil Elastase and Oxidative Stress in Atherosclerotic Plaques Using a Unimolecular Photoacoustic Probe. *Angew. Chem. Int. Ed.* **2024**, *63*, e202411840. [CrossRef]
79. Xu, M.; Sun, Q.; Wang, X.; Gao, H.; Liu, Z. Near-Infrared Absorbing BODIPY-Xanthene Hybrids for Multiplexed Photoacoustic Imaging. *Org. Lett.* **2024**, *26*, 3750–3755. [CrossRef]
80. Malacarne, M.C.; Gariboldi, M.B.; Caruso, E. BODIPYs in PDT: A Journey through the Most Interesting Molecules Produced in the Last 10 Years. *IJMS* **2022**, *23*, 10198. [CrossRef]
81. Kamkaew, A.; Lim, S.H.; Lee, H.B.; Kiew, L.V.; Chung, L.Y.; Burgess, K. BODIPY Dyes in Photodynamic Therapy. *Chem. Soc. Rev.* **2013**, *42*, 77–88. [CrossRef] [PubMed]
82. Przygoda, M.; Bartusik-Aebisher, D.; Dynarowicz, K.; Cieślar, G.; Kawczyk-Krupka, A.; Aebisher, D. Cellular Mechanisms of Singlet Oxygen in Photodynamic Therapy. *Int. J. Mol.Sci.* **2023**, *24*, 16890. [CrossRef]
83. Awuah, S.G.; You, Y. Boron Dipyrromethene (BODIPY)-Based Photosensitizers for Photodynamic Therapy. *RSC Adv.* **2012**, *2*, 11169. [CrossRef]
84. Caruso, E.; Gariboldi, M.; Sangion, A.; Gramatica, P.; Banfi, S. Synthesis, Photodynamic Activity, and Quantitative Structure-Activity Relationship Modelling of a Series of BODIPYs. *J. Photochem. Photobiol. B Biol.* **2017**, *167*, 269–281. [CrossRef] [PubMed]
85. Caruso, E.; Malacarne, M.C.; Marras, E.; Papa, E.; Bertato, L.; Banfi, S.; Gariboldi, M.B. New BODIPYs for Photodynamic Therapy (PDT): Synthesis and Activity on Human Cancer Cell Lines. *Bioorganic Med. Chem.* **2020**, *28*, 115737. [CrossRef]
86. Kim, B.; Sui, B.; Yue, X.; Tang, S.; Tichy, M.G.; Belfield, K.D. In Vitro Photodynamic Studies of a BODIPY-Based Photosensitizer. *Eur. J. Org. Chem.* **2017**, *2017*, 25–28. [CrossRef]
87. Durantini, A.M.; Greene, L.E.; Lincoln, R.; Martínez, S.R.; Cosa, G. Reactive Oxygen Species Mediated Activation of a Dormant Singlet Oxygen Photosensitizer: From Autocatalytic Singlet Oxygen Amplification to Chemicontrolled Photodynamic Therapy. *J. Am. Chem. Soc.* **2016**, *138*, 1215–1225. [CrossRef]
88. Epelde-Elezcano, N.; Martínez-Martínez, V.; Peña-Cabrera, E.; Gómez-Durán, C.F.A.; Arbeloa, I.L.; Lacombe, S. Modulation of Singlet Oxygen Generation in Halogenated BODIPY Dyes by Substitution at Their Meso Position: Towards a Solvent-Independent Standard in the Vis Region. *RSC Adv.* **2016**, *6*, 41991–41998. [CrossRef]

89. Yu, Z.; Zhou, J.; Ji, X.; Lin, G.; Xu, S.; Dong, X.; Zhao, W. Discovery of a Monoiodo Aza-BODIPY Near-Infrared Photosensitizer: In Vitro and in Vivo Evaluation for Photodynamic Therapy. *J. Med. Chem.* **2020**, *63*, 9950–9964. [CrossRef]
90. Nguyen, V.; Yim, Y.; Kim, S.; Ryu, B.; Swamy, K.M.K.; Kim, G.; Kwon, N.; Kim, C.; Park, S.; Yoon, J. Molecular Design of Highly Efficient Heavy-Atom-Free Triplet BODIPY Derivatives for Photodynamic Therapy and Bioimaging. *Angew. Chem. Int. Ed.* **2020**, *59*, 8957–8962. [CrossRef]
91. Wang, L.; Bai, J.; Qian, Y. Synthesis of a Triphenylamine BODIPY Photosensitizer with D–A Configuration and Its Application in Intracellular Simulated Photodynamic Therapy. *New J. Chem.* **2019**, *43*, 16829–16834. [CrossRef]
92. Wang, C.; Qian, Y. A Water Soluble Carbazolyl-BODIPY Photosensitizer with an Orthogonal D–A Structure for Photodynamic Therapy in Living Cells and Zebrafish. *Biomater. Sci.* **2020**, *8*, 830–836. [CrossRef]
93. Wang, Z.; Huang, L.; Yan, Y.; El-Zohry, A.M.; Toffoletti, A.; Zhao, J.; Barbon, A.; Dick, B.; Mohammed, O.F.; Han, G. Elucidation of the Intersystem Crossing Mechanism in a Helical BODIPY for Low-Dose Photodynamic Therapy. *Angew. Chem.* **2020**, *132*, 16248–16255. [CrossRef]
94. Filatov, M.A. Heavy-Atom-Free BODIPY Photosensitizers with Intersystem Crossing Mediated by Intramolecular Photoinduced Electron Transfer. *Org. Biomol. Chem.* **2020**, *18*, 10–27. [CrossRef] [PubMed]
95. Wu, W.; Cui, X.; Zhao, J. Hetero Bodipy-Dimers as Heavy Atom-Free Triplet Photosensitizers Showing a Long-Lived Triplet Excited State for Triplet–Triplet Annihilation Upconversion. *Chem. Commun.* **2013**, *49*, 9009. [CrossRef]
96. Cakmak, Y.; Kolemen, S.; Duman, S.; Dede, Y.; Dolen, Y.; Kilic, B.; Kostereli, Z.; Yildirim, L.T.; Dogan, A.L.; Guc, D.; et al. Designing Excited States: Theory-Guided Access to Efficient Photosensitizers for Photodynamic Action. *Angew. Chem. Int. Ed.* **2011**, *50*, 11937–11941. [CrossRef]
97. Nguyen, V.-N.; Yan, Y.; Zhao, J.; Yoon, J. Heavy-Atom-Free Photosensitizers: From Molecular Design to Applications in the Photodynamic Therapy of Cancer. *Acc. Chem. Res.* **2021**, *54*, 207–220. [CrossRef]
98. Zhang, W.; Ahmed, A.; Cong, H.; Wang, S.; Shen, Y.; Yu, B. Application of Multifunctional BODIPY in Photodynamic Therapy. *Dye. Pigment.* **2021**, *185*, 108937. [CrossRef]
99. Han, H.S.; Choi, K.Y. Advances in Nanomaterial-Mediated Photothermal Cancer Therapies: Toward Clinical Applications. *Biomedicines* **2021**, *9*, 305. [CrossRef]
100. Zhao, L.; Zhang, X.; Wang, X.; Guan, X.; Zhang, W.; Ma, J. Recent Advances in Selective Photothermal Therapy of Tumor. *J. Nanobiotechnol.* **2021**, *19*, 335. [CrossRef]
101. Li, J.; Wang, J.; Zhang, D.; Cui, T.; Xu, Z.; Jiang, X.-D. Synthesis, Structure and Photochemical Properties of Asymmetric NMe2-Bearing Aza-BODIPYs as Novel Photothermal Agents. *Dye. Pigment.* **2022**, *199*, 110092. [CrossRef]
102. Liu, Y.; Song, N.; Chen, L.; Liu, S.; Xie, Z. Synthesis of a Near-Infrared BODIPY Dye for Bioimaging and Photothermal Therapy. *Chem. Asian J.* **2018**, *13*, 989–995. [CrossRef]
103. Pewklang, T.; Saiyasombat, W.; Chueakwon, P.; Ouengwanarat, B.; Chansaenpak, K.; Kampaengsri, S.; Lai, R.; Kamkaew, A. Revolutionary Pyrazole-based Aza-BODIPY: Harnessing Photothermal Power Against Cancer Cells and Bacteria. *ChemBioChem* **2024**, *25*, e202300653. [CrossRef]
104. Barth, R.F.; Zhang, Z.; Liu, T. A Realistic Appraisal of Boron Neutron Capture Therapy as a Cancer Treatment Modality. *Cancer Commun.* **2018**, *38*, 36. [CrossRef]
105. Jin, W.H.; Seldon, C.; Butkus, M.; Sauerwein, W.; Giap, H.B. A Review of Boron Neutron Capture Therapy: Its History and Current Challenges. *Int. J. Part. Ther.* **2022**, *9*, 71–82. [CrossRef] [PubMed]
106. Malouff, T.D.; Seneviratne, D.S.; Ebner, D.K.; Stross, W.C.; Waddle, M.R.; Trifiletti, D.M.; Krishnan, S. Boron Neutron Capture Therapy: A Review of Clinical Applications. *Front. Oncol.* **2021**, *11*, 601820. [CrossRef]
107. Li, X.; Golberg, D. Boron Nitride Nanotubes as Drug Carriers. In *Boron Nitride Nanotubes in Nanomedicine*; Elsevier: Amsterdam, The Netherlands, 2016; pp. 79–94. ISBN 978-0-323-38945-7.
108. Xuan, S.; Zhao, N.; Zhou, Z.; Fronczek, F.R.; Vicente, M.G.H. Synthesis and in Vitro Studies of a Series of Carborane-Containing Boron Dipyrromethenes (BODIPYs). *J. Med. Chem.* **2016**, *59*, 2109–2117. [CrossRef]
109. Gibbs, J.H.; Wang, H.; Bhupathiraju, N.V.S.D.K.; Fronczek, F.R.; Smith, K.M.; Vicente, M.G.H. Synthesis and Properties of a Series of Carboranyl-BODIPYs. *J. Organomet. Chem.* **2015**, *798*, 209–213. [CrossRef]
110. Nakata, E.; Koizumi, M.; Yamashita, Y.; Onaka, K.; Sakurai, Y.; Kondo, N.; Ono, K.; Uto, Y.; Hori, H. Design, Synthesis and Destructive Dynamic Effects of BODIPY-Containing and Curcuminoid Boron Tracedrugs for Neutron Dynamic Therapy. *Anticancer. Res.* **2011**, *31*, 2477–2481.
111. Kalot, G.; Godard, A.; Busser, B.; Pliquett, J.; Broekgaarden, M.; Motto-Ros, V.; Wegner, K.D.; Resch-Genger, U.; Köster, U.; Denat, F.; et al. Aza-BODIPY: A New Vector for Enhanced Theranostic Boron Neutron Capture Therapy Applications. *Cells* **2020**, *9*, 1953. [CrossRef]
112. Bellomo, C.; Zanetti, D.; Cardano, F.; Sinha, S.; Chaari, M.; Fin, A.; Maranzana, A.; Núñez, R.; Blangetti, M.; Prandi, C. Red Light-Emitting Carborane-BODIPY Dyes: Synthesis and Properties of Visible-Light Tuned Fluorophores with Enhanced Boron Content. *Dye. Pigment.* **2021**, *194*, 109644. [CrossRef]

113. Zhang, T.; Ma, C.; Sun, T.; Xie, Z. Unadulterated BODIPY Nanoparticles for Biomedical Applications. *Coord. Chem. Rev.* **2019**, *390*, 76–85. [CrossRef]
114. Lin, W.; Colombani-Garay, D.; Huang, L.; Duan, C.; Han, G. Tailoring Nanoparticles Based on Boron Dipyrromethene for Cancer Imaging and Therapy. *WIREs Nanomed. Nanobiotechnol.* **2020**, *12*, e1627. [CrossRef]
115. Wang, X.; Jiang, Z.; Liang, Z.; Wang, T.; Chen, Y.; Liu, Z. Discovery of BODIPY J-Aggregates with Absorption Maxima beyond 1200 Nm for Biophotonics. *Sci. Adv.* **2022**, *8*, eadd5660. [CrossRef]
116. Liu, Z.; Jiang, Z.; Yan, M.; Wang, X. Recent Progress of BODIPY Dyes With Aggregation-Induced Emission. *Front. Chem.* **2019**, *7*, 712. [CrossRef]
117. Descalzo, A.B.; Ashokkumar, P.; Shen, Z.; Rurack, K. On the Aggregation Behaviour and Spectroscopic Properties of Alkylated and Annelated Boron-Dipyrromethene (BODIPY) Dyes in Aqueous Solution. *ChemPhotoChem* **2020**, *4*, 120–131. [CrossRef]
118. Kumar, P.P.P.; Yadav, P.; Shanavas, A.; Neelakandan, P.P. Aggregation Enhances Luminescence and Photosensitization Properties of a Hexaiodo-BODIPY. *Mater. Chem. Front.* **2020**, *4*, 965–972. [CrossRef]
119. Salis, F.; Descalzo, A.B.; Benito-Peña, E.; Moreno-Bondi, M.C.; Orellana, G. Highly Fluorescent Magnetic Nanobeads with a Remarkable Stokes Shift as Labels for Enhanced Detection in Immunoassays. *Small* **2018**, *14*, 1703810. [CrossRef]
120. Rahman, A.; Praveen Kumar, P.P.; Yadav, P.; Goswami, T.; Shanavas, A.; Ghosh, H.N.; Neelakandan, P.P. Gold–BODIPY Nanoparticles with Luminescence and Photosensitization Properties for Photodynamic Therapy and Cell Imaging. *ACS Appl. Nano Mater.* **2022**, *5*, 6532–6542. [CrossRef]
121. Kumar, P.P.P.; Rahman, A.; Goswami, T.; Ghosh, H.N.; Neelakandan, P.P. Fine-Tuning Plasmon-Molecule Interactions in Gold-BODIPY Nanocomposites: The Role of Chemical Structure and Noncovalent Interactions. *ChemPlusChem* **2021**, *86*, 87–94. [CrossRef]
122. Kumar, P.P.P. A Multimode Detection Platform for Biothiols Using BODIPY Dye-Conjugated Gold Nanoparticles. *Colorants* **2024**, *3*, 214–228. [CrossRef]
123. Kumar, P.P.P.; Yadav, P.; Shanavas, A.; Thurakkal, S.; Joseph, J.; Neelakandan, P.P. A Three-Component Supramolecular Nanocomposite as a Heavy-Atom-Free Photosensitizer. *Chem. Commun.* **2019**, *55*, 5623–5626. [CrossRef]
124. Praveen Kumar, P.P.; Kaur, N.; Shanavas, A.; Neelakandan, P.P. Nanomolar Detection of Biothiols via Turn-ON Fluorescent Indicator Displacement. *Analyst* **2020**, *145*, 851–857. [CrossRef]
125. Li, Z.; Zheng, M.; Guan, X.; Xie, Z.; Huang, Y.; Jing, X. Unadulterated BODIPY-Dimer Nanoparticles with High Stability and Good Biocompatibility for Cellular Imaging. *Nanoscale* **2014**, *6*, 5662–5665. [CrossRef] [PubMed]
126. Liu, Y.; Song, N.; Chen, L.; Xie, Z. Triple-BODIPY Organic Nanoparticles with Particular Fluorescence Emission. *Dye. Pigment.* **2017**, *147*, 241–245. [CrossRef]
127. Lin, W.; Sun, T.; Xie, Z.; Gu, J.; Jing, X. A Dual-Responsive Nanocapsule via Disulfide-Induced Self-Assembly for Therapeutic Agent Delivery. *Chem. Sci.* **2016**, *7*, 1846–1852. [CrossRef] [PubMed]
128. Zhang, W.; Lin, W.; Pei, Q.; Hu, X.; Xie, Z.; Jing, X. Redox-Hypersensitive Organic Nanoparticles for Selective Treatment of Cancer Cells. *Chem. Mater.* **2016**, *28*, 4440–4446. [CrossRef]
129. Lin, W.; Zhang, W.; Sun, T.; Gu, J.; Xie, Z.; Jing, X. Effect of Molecular Structure on Stability of Organic Nanoparticles Formed by Bodipy Dimers. *Langmuir* **2016**, *32*, 9575–9581. [CrossRef]
130. Huang, L.; Li, Z.; Zhao, Y.; Zhang, Y.; Wu, S.; Zhao, J.; Han, G. Ultralow-Power Near Infrared Lamp Light Operable Targeted Organic Nanoparticle Photodynamic Therapy. *J. Am. Chem. Soc.* **2016**, *138*, 14586–14591. [CrossRef]
131. Huang, L.; Li, Z.; Zhao, Y.; Yang, J.; Yang, Y.; Pendharkar, A.I.; Zhang, Y.; Kelmar, S.; Chen, L.; Wu, W.; et al. Enhancing Photodynamic Therapy through Resonance Energy Transfer Constructed Near-Infrared Photosensitized Nanoparticles. *Adv. Mater.* **2017**, *29*, 1604789. [CrossRef]
132. Naim, K.; Nair, S.T.; Yadav, P.; Shanavas, A.; Neelakandan, P.P. Supramolecular Confinement within Chitosan Nanocomposites Enhances Singlet Oxygen Generation. *ChemPlusChem* **2018**, *83*, 418–422. [CrossRef] [PubMed]
133. Tang, Q.; Xiao, W.; Huang, C.; Si, W.; Shao, J.; Huang, W.; Chen, P.; Zhang, Q.; Dong, X. pH-Triggered and Enhanced Simultaneous Photodynamic and Photothermal Therapy Guided by Photoacoustic and Photothermal Imaging. *Chem. Mater.* **2017**, *29*, 5216–5224. [CrossRef]
134. Lin, W.; Zhang, W.; Liu, S.; Li, Z.; Hu, X.; Xie, Z.; Duan, C.; Han, G. Engineering pH-Responsive BODIPY Nanoparticles for Tumor Selective Multimodal Imaging and Phototherapy. *ACS Appl. Mater. Interfaces* **2019**, *11*, 43928–43935. [CrossRef]
135. Zou, J.; Wang, P.; Wang, Y.; Liu, G.; Zhang, Y.; Zhang, Q.; Shao, J.; Si, W.; Huang, W.; Dong, X. Penetration Depth Tunable BODIPY Derivatives for pH Triggered Enhanced Photothermal/Photodynamic Synergistic Therapy. *Chem. Sci.* **2019**, *10*, 268–276. [CrossRef] [PubMed]
136. Villalobos Gutiérrez, P.; Muñoz Carrillo, J.; Sandoval Salazar, C.; Viveros Paredes, J.; Gutiérrez Coronado, O. Functionalized Metal Nanoparticles in Cancer Therapy. *Pharmaceutics* **2023**, *15*, 1932. [CrossRef]

137. Malacarne, M.C.; Caruso, E.; Gariboldi, M.B.; Marras, E.; Della Bitta, G.; Santoro, O.; Simm, A.; Li, R.; Ferguson, C.T.J. Evaluation of Nanoparticles Covalently Bound with BODIPY for Their Photodynamic Therapy Applicability. *Int. J. Mol. Sci.* **2024**, *25*, 3187. [CrossRef] [PubMed]
138. Topel, S.D.; Topel, Ö.; Bostancıoğlu, R.B.; Koparal, A.T. Synthesis and Characterization of Bodipy Functionalized Magnetic Iron Oxide Nanoparticles for Potential Bioimaging Applications. *Colloids Surf. B Biointerfaces* **2015**, *128*, 245–253. [CrossRef]
139. Kim, C.K.; Ghosh, P.; Pagliuca, C.; Zhu, Z.-J.; Menichetti, S.; Rotello, V.M. Entrapment of Hydrophobic Drugs in Nanoparticle Monolayers with Efficient Release into Cancer Cells. *J. Am. Chem. Soc.* **2009**, *131*, 1360–1361. [CrossRef]
140. Sun, L.; Liu, H.; Ye, Y.; Lei, Y.; Islam, R.; Tan, S.; Tong, R.; Miao, Y.-B.; Cai, L. Smart Nanoparticles for Cancer Therapy. *Sig Transduct. Target. Ther.* **2023**, *8*, 418. [CrossRef]
141. Wang, B.; Hu, S.; Teng, Y.; Chen, J.; Wang, H.; Xu, Y.; Wang, K.; Xu, J.; Cheng, Y.; Gao, X. Current Advance of Nanotechnology in Diagnosis and Treatment for Malignant Tumors. *Sig Transduct. Target. Ther.* **2024**, *9*, 200. [CrossRef]
142. Chehelgerdi, M.; Chehelgerdi, M.; Allela, O.Q.B.; Pecho, R.D.C.; Jayasankar, N.; Rao, D.P.; Thamaraikani, T.; Vasanthan, M.; Viktor, P.; Lakshmaiya, N.; et al. Progressing Nanotechnology to Improve Targeted Cancer Treatment: Overcoming Hurdles in Its Clinical Implementation. *Mol. Cancer* **2023**, *22*, 169. [CrossRef] [PubMed]
143. Gavas, S.; Quazi, S.; Karpiński, T.M. Nanoparticles for Cancer Therapy: Current Progress and Challenges. *Nanoscale Res. Lett.* **2021**, *16*, 173. [CrossRef] [PubMed]

Disclaimer/Publisher's Note: The statements, opinions and data contained in all publications are solely those of the individual author(s) and contributor(s) and not of MDPI and/or the editor(s). MDPI and/or the editor(s) disclaim responsibility for any injury to people or property resulting from any ideas, methods, instructions or products referred to in the content.